

RESEARCH ARTICLE

10.1029/2019JD030627

Key Points:

- Observations of ClNO_2 and Cl_2 show that even under acidic conditions, the uptake of ClNO_2 proceeds much slower than previously reported
- The availability of particulate chloride in acidic aerosols and particle size limit the efficiency of the conversion of ClNO_2 to Cl_2
- Despite a slower reaction, ClNO_2 reactions on aerosol can be a significant source of Cl_2 in polluted regions

Supporting Information:

- Supporting Information S1

Correspondence to:

J. A. Thornton,
thornton@atmos.washington.edu

Citation:

Haskins, J. D., Lee, B. H., Lopez-Hilfiker, F. D., Peng, Q., Jaeglé, L., Reeves, J. M., et al. (2019). Observational constraints on the formation of Cl_2 from the reactive uptake of ClNO_2 on aerosols in the polluted marine boundary layer. *Journal of Geophysical Research: Atmospheres*, 124, 8851–8869. <https://doi.org/10.1029/2019JD030627>











Received 13 MAR 2019

Accepted 12 JUN 2019

Accepted article online 13 JUL 2019

Published online 13 AUG 2019

Observational Constraints on the Formation of Cl_2 From the Reactive Uptake of ClNO_2 on Aerosols in the Polluted Marine Boundary Layer

Jessica D. Haskins¹ , Ben H. Lee¹ , Felipe D. Lopez-Hilfiker^{1,2}, Qiaoyun Peng¹, Lyatt Jaeglé¹ , J. Michael Reeves³, Jason C. Schroder^{4,5} , Pedro Campuzano-Jost^{4,5} , Dorothy Fibiger^{4,6,7} , Erin E. McDuffie^{4,6,5,8} , José L. Jiménez^{4,5} , Steven S. Brown^{6,5} , and Joel A. Thornton¹ 

¹Department of Atmospheric Sciences, University of Washington, Seattle, WA, USA, ²Now at Tofwerk AG, Thun, Switzerland, ³Earth Observing Laboratory, National Corporation for Atmospheric Research, Boulder, CO, USA,

⁴Cooperative Institute for Research in Environmental Science, University of Colorado, Boulder, CO, USA,

⁵Department of Chemistry, University of Colorado Boulder, Boulder, CO, USA, ⁶Chemical Sciences Division, NOAA Earth System Research Laboratory, Boulder, CO, USA, ⁷Now at California Air Resources Board, Sacramento, CA, USA,

⁸Now at the Department of Physics and Atmospheric Science, Dalhousie University, Halifax, Nova Scotia, Canada

Abstract We use observations from the 2015 Wintertime Investigation of Transport, Emissions, and Reactivity (WINTER) aircraft campaign to constrain the proposed mechanism of Cl_2 production from ClNO_2 reaction in acidic particles. To reproduce Cl_2 concentrations observed during WINTER with a chemical box model that includes ClNO_2 reactive uptake to form Cl_2 , the model required the ClNO_2 reaction probability, γ (ClNO_2), to range from 6×10^{-6} to 7×10^{-5} , with a mean value of 2.3×10^{-5} ($\pm 1.8 \times 10^{-5}$). These field-determined γ (ClNO_2) are more than an order of magnitude lower than those determined in previous laboratory experiments on acidic surfaces, even when calculated particle pH is ≤ 2 . We hypothesize this is because thick salt films in the laboratory enhanced the reactive uptake ClNO_2 compared to that which would occur in submicron aerosol particles. Using the reacto-diffusive length-scale framework, we show that the field and laboratory observations can be reconciled if the net aqueous-phase reaction rate constant for ClNO_2 (aq) + Cl^- (aq) in acidic particles is on the order of 10^4 s^{-1} . We show that wet particle diameter and particulate chloride mass together explain 90% of the observed variance in the box model-derived γ (ClNO_2), implying that the availability of chloride and particle volume limit the efficiency of the reaction. Despite a much lower conversion of ClNO_2 into Cl_2 , this mechanism can still be responsible for the nocturnal formation of 10–20 pptv of Cl_2 in polluted regions, yielding an atmospherically relevant concentration of Cl atoms the following morning.

1. Introduction

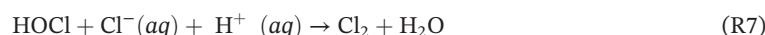
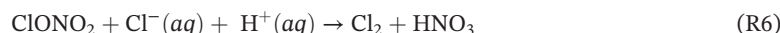
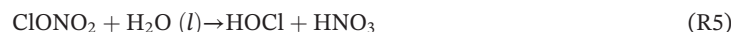
The largest source of inorganic chlorine gases ($\text{Cl}_y = \text{HCl} + \text{ClNO}_2 + \text{HOCl} + 2\text{Cl}_2$) to the troposphere is from the volatilization of particle chloride (pCl^-) from sea salt aerosols (SSA; Graedel & Keene, 1995; Finlayson-Pitts et al., 1989). In polluted regions, reactions of nitrogen oxides ($\text{NO}_x = \text{NO}_2 + \text{NO}$) and volatile organic compounds (VOCs) can enhance the liberation of chloride from particles. This chlorine activation impacts air quality by increasing oxidant sources through the formation of Cl-atom precursors such as nitryl chloride (ClNO_2) and molecular chlorine (Cl_2), which rapidly photolyze during the day (Saiz-Lopez & von Glasow, 2012; Schmidt et al., 2016; Sherwen et al., 2016; Simpson et al., 2015; von Glasow et al., 2004).

Cl atoms are highly reactive toward ozone (O_3) and VOCs, and have rate coefficients orders of magnitude larger than the hydroxyl radical (OH) for reactions with most alkanes. Although concentrations of Cl atoms in the troposphere are orders of magnitude lower than that of OH, their high reaction rates with O_3 and VOCs make Cl atoms an atmospherically important oxidizer. Several recent observational studies have concluded that in summertime coastal urban areas, reactions with Cl atoms dominated the early morning oxidation of alkanes before ~ 10 a.m., surpassing OH reactions and that 15–25% of the total daily alkane oxidation was driven by Cl atoms (Bannan et al., 2015; Riedel et al., 2012). On a global scale, Wang et al. (2018) estimated that Cl atoms were responsible for 1% of the global oxidation of methane, and 20% of

ethane, among other alkanes. Ultimately, because of the importance of Cl atoms to the overall oxidant budget in the lower troposphere, sources of Cl atoms are important to constrain.

ClNO₂ production has recently represented a major focus of research into tropospheric Cl-atom sources. Over the course of an entire day, photolysis of ClNO₂ could account for 45% of the integrated Cl atom production in polluted offshore regions of the United States (Riedel et al., 2012, 2014), where [ClNO₂] can reach ~1 ppbv. Some studies in rural northern China, where the direct emission of photolytic chlorine containing compounds from coal-fired power plants is larger, the contribution of ClNO₂ to the total Cl-atom budget can be smaller, ranging from 16–21% (Liu et al., 2017; Liu et al., 2018), though this may not be the case for other regions.

Prior to the discovery of ClNO₂ production in the troposphere, past work on tropospheric Cl-atom sources often focused on BrCl or Cl₂, which are produced from multiphase chemistry or emitted directly from industrial processes (Faxon et al., 2015; Finley & Saltzman, 2006; Keene et al., 2007; Lawler et al., 2011; Lee, Lopez-Hilfiker, Schroder, et al., 2018; Liao et al., 2014; Pszenny et al., 1993; Pszenny et al., 2004; Riedel et al., 2012; Spicer et al., 1998; Tanaka et al., 2000;). In situ production of tropospheric Cl₂ has been proposed to occur via several mechanisms, including the daytime reaction of OH on chlorine-containing particle surfaces (Knipping et al., 2000; Laskin et al., 2012), snowpack chemistry (Custard et al., 2017; Pratt et al., 2013), and reactive uptake of hypochlorous acid (HOCl) and chlorine nitrate (ClONO₂) on SSA (Vogt et al., 1996). Reported tropospheric mixing ratios of Cl₂ tend to be <100 pptv, and typically on the order of 10 pptv (Faxon et al., 2015; Finley & Saltzman, 2006; Keene et al., 2007; Lawler et al., 2011; Pszenny et al., 1993; Pszenny et al., 2004; Riedel et al., 2012; Spicer et al., 1998;).



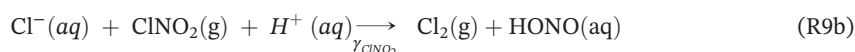
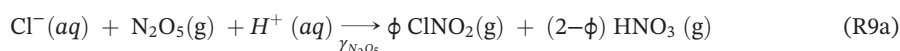
Cl atoms can react with O₃ to form chlorine monoxide (ClO) via R1, which can subsequently react with the hydroperoxyl radical (HO₂) or nitrogen dioxide (NO₂) to form HOCl or ClONO₂, respectively ((R2) and (R3)). Because Cl atoms are highly reactive with VOCs, more so than with O₃, and the loss of ClO to nitric oxide (NO) via (R4) can dominate ClO's fate in polluted regions (Riedel et al., 2012), the availability of ClO can be a limiting step in the formation of HOCl and ClONO₂. If formed, ClONO₂ can undergo conversion to HOCl (R5), and either HOCl or ClONO₂ can form Cl₂ via acid-catalyzed multiphase chemistry ((R6) and (R7)). Or HOCl and ClONO₂ can undergo photolysis, which would recycle the single Cl-atom, instead of liberating a second Cl-atom from the particle (Pechtl & von Glasow, 2007; Vogt et al., 1996). In total, these reactions can form an autocatalytic cycle liberating reactive Cl atoms from the particle phase. In polluted continental outflow, Riedel et al. (2012) found that these reactions only enhanced Cl₂ in the early morning hours, initiated by the photolysis of ClNO₂, when the NO/NO₂ ratio was low enough that (R4) did not suppress the formation of HOCl and ClONO₂, which otherwise lead to the production of a few parts per trillion volume of Cl₂ at night.

Using tropospheric observations of Cl₂ and HOCl, Lawler et al. (2011) estimated a reaction probability for HOCl, γ (HOCl) of 1.7×10^{-3} to best explain observed Cl₂ levels and the rate of evening conversion of HOCl to Cl₂ in a pristine marine environment. This field-derived γ (HOCl) value is an order of magnitude above those inferred from laboratory experiments using acidified SSA by Pratte and Rossi (2006). γ (HOCl) values from Lawler et al. (2011) imply nearly complete conversion of HOCl into Cl₂ over a night at typical tropospheric temperatures and aerosol surface area density, while those from Pratte and Rossi (2006) imply 5 to

10% conversion. Ultimately, these studies suggest that conversion of HOCl to Cl₂ could be significant in the atmosphere but highlight the differences in field and laboratory estimates of such uptake processes.

Riedel et al. (2012) hypothesized that the fate of ClONO₂ on aerosol particles was particularly important in polluted regions, since even a slow conversion of ClONO₂ to HOCl via (R5) and subsequent conversion to Cl₂ via (R7), could lead to production of ~40 pptv of Cl₂ at night, even if ClONO₂ production was slowed by NO during the preceding day. Breton et al., (2018) reported ClONO₂ measurements in the troposphere with concentrations peaking at night and being sustained around 15 pptv at a semirural site northwest of Beijing. Although laboratory constraints on the heterogeneous reaction of ClONO₂ with HCl to form Cl₂ exist under stratospheric conditions (e.g., Hanson & Ravishankara, 1994), few laboratory measurements at typical tropospheric temperatures exist. These studies suggest a wide range in the efficiency of uptake on particles or surfaces containing NaCl with γ (ClONO₂) estimates ranging from 4.6×10^{-3} to 0.14, though all agree that the yield of Cl₂ is 100% (Burkholder et al., 2015).

Another mechanism for in situ Cl₂ production was proposed in Roberts et al. (2008), where the nocturnal production of ClNO₂ from dinitrogen pentoxide (N₂O₅) uptake leads to Cl₂ via reaction on acidic aerosols (R9) following a mechanism analogous to the formation of Br₂ from BrNO₂ on Br⁻ containing substrates.



In a series of experiments, they showed that the uptake of ClNO₂ proceeded with 60–100% efficiency resulting in ~1 ppbv of Cl₂ for ~1–1.5 ppbv of ClNO₂ reacted, when ClNO₂ was passed over a film of deliquesced oxalic acid and NaCl (pH ~1.8). On a variety of acidic surfaces with pH ≤ 2, they estimated γ (ClNO₂) values of 6×10^{-3} ($\pm 2 \times 10^{-3}$) with [Cl⁻] as low as 0.05 M, while on less acidic surfaces, they found that ClNO₂ was relatively unreactive with γ (ClNO₂) = 0.3×10^{-6} to 5×10^{-6} (Roberts et al., 2008, 2009). Additional studies have investigated the uptake of ClNO₂ without observing specific products or controlling pH, and have shown that γ (ClNO₂) on pure water is <10⁻⁵ and on the order of 10⁻⁶ on low-concentration halide surfaces, with no temperatures dependence between 177 and 291 K (Behnke et al., 1997; Burkholder et al., 2015; Frenzel et al., 1998; George et al., 1995; Schweitzer et al., 1998).

Given that ClNO₂ has routinely been observed in the troposphere exceeding 1 ppbv (Osthoff et al., 2008; Thornton et al., 2010; Mielke et al., 2011, 2013; Phillips et al., 2012; Riedel et al., 2012, 2013; Tham et al., 2014; Bannan et al., 2015; Faxon et al., 2015; Wang et al., 2017; Haskins et al., 2018; Yun et al., 2018), this production channel (R9) suggests significant Cl₂ production, on the order of 1 ppbv. Since, concentrations of ClNO₂ can be an order of magnitude larger than HOCl concentrations in polluted regions, and the literature values for γ (ClNO₂) on acidic aerosol are larger than γ (HOCl), production of Cl₂ from ClNO₂ uptake is potentially far greater than from HOCl. Therefore, this mechanism of Cl₂ production would be essential to include in models to simulate tropospheric production of Cl atoms and the oxidative capacity of the atmosphere.

Despite the implication that ClNO₂ uptake could contribute up to 1 ppbv of Cl₂, the only recent measurements observing tropospheric Cl₂ exceeding ~150 pptv in the troposphere were attributed to large, direct emissions of Cl₂ from coal-fired power plants in China, occurring in the daytime, when ClNO₂ chemistry is not prominent (Liu et al., 2017; Liu et al., 2018). All other recent measurements of Cl₂ in the troposphere have shown concentrations on the order of 10–20 pptv, with maxima at night, even with simultaneous ClNO₂ observations >1 ppbv (Finley & Saltzman, 2006; Haskins et al., 2018; Lawler et al., 2011; Riedel et al., 2012;). Although the pioneering measurements of Keene et al. (1993) and Spicer et al. (1998) showed Cl₂* (Cl₂* = Cl₂ + HOCl) in excess of 120 pptv peaking at night, those high concentrations of Cl₂* are thought to be driven more by HOCl than Cl₂ at night (Pszenny et al., 1993). Furthermore, Wang et al. (2018) significantly overestimated nighttime aircraft observations of Cl₂ during the 2015 Wintertime Investigation of Transportation, Emissions, and Reactivity (WINTER) campaign, using the global chemistry model, GEOS-Chem, when including Cl₂ production from ClNO₂ uptake on acidic aerosols. Therefore, observations suggest that Cl₂ production from heterogeneous ClNO₂ reaction on acidic particles either

occurs with a lower efficiency in the atmosphere than was measured in the laboratory, that Cl_2 production from ClNO_2 in the atmosphere is limited by a lack of aerosol having both sufficient acidity and pCl^- , or no observations reported to date have been made in areas where this chemistry is relevant.

Recent studies have shown that submicron aerosols across the globe are acidic, with pH ranging from -0.5 to 3 , suggesting that the conditions for efficient ClNO_2 uptake and Cl_2 production are often satisfied, at least in submicron aerosols (Guo et al., 2015; Guo et al., 2016; Guo et al., 2017). However, a large majority of the chloride mass is expected in the supermicron ($>1\ \mu\text{m}$) range (Keene et al., 1999). This supermicron SSA is more likely to be present in less acidic particles and is less likely to be internally mixed than acidic submicron aerosols. Indeed, a few studies determined that the uptake of ClNO_2 was unlikely as a source of their observed Cl_2 since thermodynamic calculations showed the aerosols sampled had $\text{pH} > 2$, which was not acidic enough to catalyze efficient ClNO_2 uptake (Mielke et al., 2011; Riedel et al., 2012, 2013). However, Guo et al. (2016) showed that submicron particles offshore from New York City during WINTER were predicted to have $\text{pH} \leq 2$. Furthermore, Haskins et al. (2018) showed that both predicted and observed submicron pCl^- was sufficient to promote chloride activation chemistry. Elevated concentrations of gas-phase HCl and ClNO_2 in the marine boundary layer indicated internally mixed chloride was activated via heterogeneous chemistry, with submicron aerosols present that contained chloride and had low calculated pH at the time of aircraft sampling. Therefore, the condition of coexisting aerosol acidity and available pCl^- necessary to catalyze ClNO_2 uptake does appear exist in the troposphere, and the WINTER campaign provides an opportunity to evaluate laboratory parameterizations of Cl_2 formation from ClNO_2 uptake.

In this work, we use WINTER observations of Cl_2 , ClNO_2 , HOCl , N_2O_5 , HNO_3 , O_3 , NO_2 , pCl^- , among others in a box model to derive an upper limit to the reaction probability of ClNO_2 , $\gamma(\text{ClNO}_2)$, needed to explain the Cl_2 concentrations observed in specific plumes where the two are highly correlated. We use a reacto-diffusive length framework (Hansen et al., 1994) to reconcile differences between these field-derived reaction probabilities on ambient aerosol with those derived in the laboratory using macroscopic salt films. Observed correlations between the box model-derived $\gamma(\text{ClNO}_2)$ and parameters such as relative humidity, aerosol pH, aerosol diameter, and pCl^- concentrations are evaluated, and we present a simple empirical parameterization of Cl_2 production from ClNO_2 reactive uptake based on these observed relationships.

2. Methods

2.1. WINTER Campaign and Observations

The WINTER campaign took place in February and March 2015 using the NSF/NCAR C-130 aircraft. This campaign sampled a broad suite of chemical compounds in 13 flights over the eastern United States during both day and night above marine, rural, and highly populated areas. Observations of halogen trace gases, reactive nitrogen oxides, O_3 , aerosol composition, and aerosol size distributions were made, some with duplicate techniques. A summary of the instrument accuracy, detection limit, measurement frequency, and operational technique references for the observations used in this work from the WINTER campaign and additional instrument details are given in the supporting information. All observations presented in this work are 10-s averages of the data collected at 1–2 Hz to improve the signal to noise ratio while maintaining temporal resolution. More information on the WINTER campaign and instrumentation can be found in papers published as a special collection (Guo et al., 2016; Salmon et al., 2017; Fibiger et al., 2018; Jaeglé et al., 2018; Haskins et al., 2018; Kenagy et al., 2018; Lee, Lopez-Hilfiker, Schroder, et al., 2018; Lee, Lopez-Hilfiker, Veres, et al., 2018; McDuffie, Fibiger, Dubé, Lopez Hilfiker, et al., 2018; McDuffie, Fibiger, Dubé, Lopez-Hilfiker, et al., 2018; Ren et al., 2018; Salmon et al., 2018; Schroder et al., 2018; Sullivan et al., 2019).

The Ultra High Sensitivity Aerosol Spectrometer (UHSAS) was used to measure dry submicron particle surface area density during WINTER. Wet aerosol surface area (cm^2/cm^3) and volume (cm^3/cm^3) densities are calculated by summing the product of the dry surface area or volume density by relative humidity dependent, hygroscopic growth factors for particles $<1\ \mu\text{m}$ in diameter. Surface and volume growth factors were obtained using the E-AIM model, assuming pure ammonium nitrate submicron particles and no solid formation. This calculation does not consider the impact of aerosol organics on hygroscopic growth, and a comparison between the two approaches for calculating diameter growth factors during WINTER is presented in Figure S1 of McDuffie, Fibiger, Dubé, Lopez-Hilfiker, et al. (2018). For some plumes of interest, the

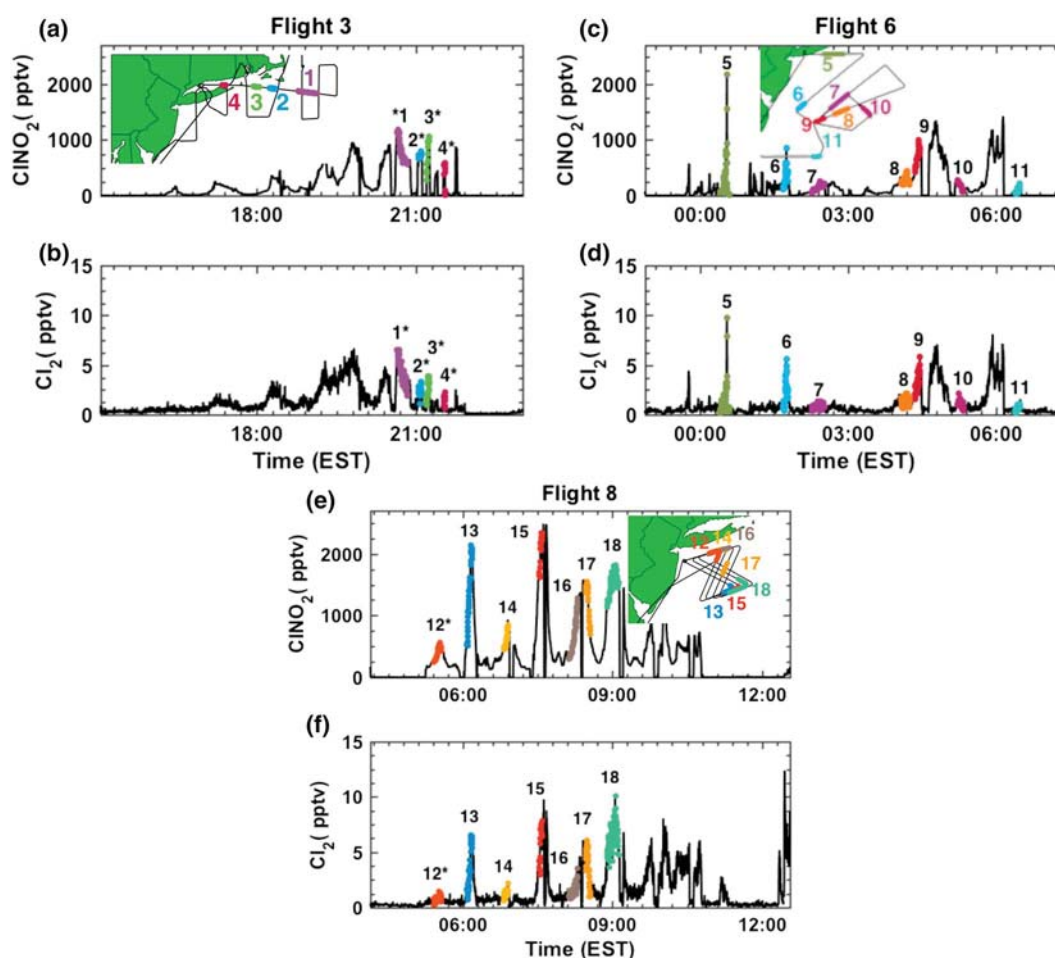


Figure 1. Time series of ClNO_2 and Cl_2 from Research Flight 3 on 7 February 2015 (a, b), Research Flight 6 on 23 February 2015 (c, d), and Research Flight 8 on 1 March 2015 (e, f) with inlaid flight tracks off the coast of New York City, highlighting the 18 plumes (numbered for reference) used in the box model analysis presented in this work. Enhancements in Cl_2 and ClNO_2 not highlighted are those where all measurements necessary for the box model analysis were not available, were during daytime, in-cloud, or where correlations are caused by plane altitude changes. In all figures, asterisks denote plumes where wet aerosol surface area was estimated using the Aerosol Mass Spectrometer total mass. See text for details.

UHSAS was not functioning. So a linear model was used to predict the wet aerosol surface area concentration using a parameterization based on the Aerosol Mass Spectrometer (AMS) total submicron mass concentration, derived from collocated measurements when both instruments were sampling. Details on this calculation and the aerosol growth factors can be found in the supporting information. The plumes where aerosol surface area concentration is estimated using this parameterization are denoted in all figures and tables with an asterisk.

To investigate the nocturnal uptake of ClNO_2 and subsequent production of Cl_2 , we examine three nighttime flights that sampled the polluted marine boundary layer downwind of New York City. Figure 1 shows a time series of the concentrations of Cl_2 and ClNO_2 from each of these flights and an inlaid map of the flight track, highlighting 18 plumes we examine here. These plumes do not include those where ClNO_2 and Cl_2 are correlated due to plane altitude changes, or observations that occurred before sunset or after sunrise when photolytic loss of Cl_2 and ClNO_2 are important. More information on plumes where these compounds appear correlated in time, but are not included due to these factors, can be found in the supporting information. General trends in Cl_2 , ClNO_2 , HOCl , and HCl concentrations observed throughout the WINTER campaign can be found in Haskins et al. (2018), and trends in these halogen species observed within power-plant plumes during WINTER can be found in Lee, Lopez-Hilfiker, Schroder, et al. (2018).

As shown in Figure 2, Cl_2 was positively correlated with ClNO_2 ($r^2 = 0.88$), and with HOCl to a lesser degree ($r^2 = 0.52$), implying Cl_2 , like ClNO_2 , is formed by nocturnal heterogeneous chemistry, rather than direct

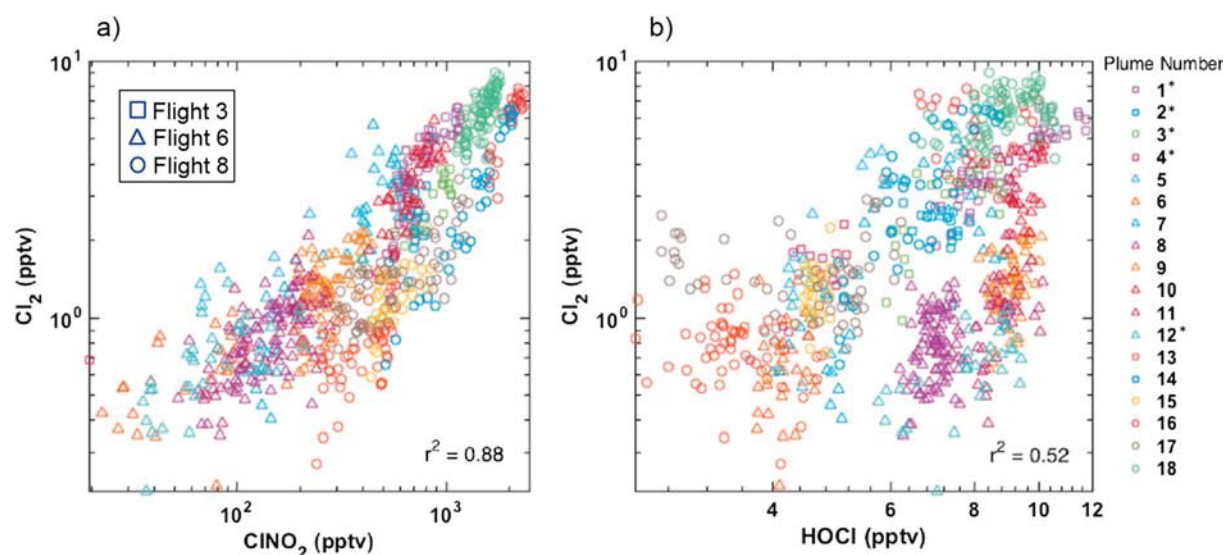


Figure 2. Scatterplots of measured Cl_2 as a function of (a) ClNO_2 and (b) HOCl within each plume using 10-s averages colored by plume number with markers indicating flight number.

emission. Although these plumes are downwind of several significant anthropogenic sources of Cl_2 , as reported to the Environmental Protection Agency, these specific plumes of Cl_2 do not show a pattern of direct emission from a point source, which Riedel et al. (2012) demonstrates is distinguishable in a time series from a pattern of in situ formation, since plumes influenced by direct emission of Cl_2 are not expected to show correlation with ClNO_2 . Inlet and inner instrument conversion of HOCl or ClNO_2 to Cl_2 is unlikely, as Lee, Lopez-Hilfiker, Veres, et al., et al. (2018) showed that conversion of directly injected, isotopically labeled N_2O_5 to ClNO_2 yielded only of 1 pptv ClNO_2 per 100 pptv of N_2O_5 during WINTER. The assumption that all Cl_2 plumes are from in situ production via ClNO_2 uptake alone, rather than uptake of HOCl or instrument artifacts will be discussed below in section 3.2, but would tend to bias our estimates of γ (ClNO_2) high relative to the true value. While we cannot rule out that the simultaneous uptake of ClNO_2 and HOCl in these plumes is contributing to the elevated Cl_2 concentrations, observations in Figure 2 suggest that the production and loss of Cl_2 is more highly correlated with ClNO_2 than with HOCl .

2.2. Aerosol Thermodynamics and Multiphase Chemical Box Model

The aerosol thermodynamics model ISORROPIA II was used to calculate submicron particle pH and liquid water content during WINTER as described in Haskins et al. (2018) and Guo et al. (2016). Previous evaluations of the gas-particle partitioning of chlorine and nitrate predicted by ISORROPIA II against the WINTER data set provide confidence in the ISORROPIA II prediction of bulk average pH and liquid water content used in this work for submicron particles (Guo et al., 2016; Haskins et al., 2018; Shah et al., 2018). Given the low temperatures observed during WINTER, partitioning of HNO_3 into particles was high, thereby driving submicron particle pH low for much of the campaign (Guo et al., 2016). In all plumes where Cl_2 and ClNO_2 were simultaneously elevated, calculated submicron particle pH was <2 , so comparison of this chemistry at higher pH is not possible with this data set.

A simple zero-dimensional box model was developed to simulate the nocturnal chemical evolution of an air parcel at constant temperature, pressure, and relative humidity. Table 1 summarizes the reactions included in this model and their rate coefficient expressions. The model was run from 5 p.m. local time, considered the onset of N_2O_5 production, for 16.5 hr until 9:30 a.m. local time on the following day, for each of the identified plumes. Assuming loss due only to N_2O_5 formation (i.e., no deposition or dilution), the initial concentrations of O_3 and NO_2 at sunset were iteratively adjusted until their modeled loss matched the observations of NO_2 and O_3 at the time the C-130 aircraft intercepted the plume within measurement uncertainty, similar to previous studies of nocturnal reactive nitrogen chemistry (Brown et al., 2003; Thornton et al., 2010; Mielke et al., 2011; Wagner et al., 2013; Phillips et al., 2016; McDuffie, Fibiger, Dubé, Lopez-Hilfiker, et al., 2018; Tham et al., 2018). The amount of reacted O_3 and NO_2 sets a maximum amount of N_2O_5

Table 1
Reactions and Rate Constants Included in 0-D Box Model

Reaction no.	Reaction	Rate coefficient expression	Reference
		($\text{cm}^3 \cdot \text{molecules}^{-1} \cdot \text{s}^{-1}$)	
R10	$\text{NO}_2 + \text{O}_3 \xrightarrow{k_{10}} \text{NO}_3 + \text{O}_2$	$k_{10} = 1.2e^{-13} \exp(-2,450/T)$	Sander et al. (2003)
R11f	$\text{NO}_3 + \text{NO}_2 \xrightleftharpoons[k_{11r}]{k_{11f}} \text{N}_2\text{O}_5$	$k_{11f} = (k_0/k_\infty) * F / (k_0 + k_\infty)$	DeMore et al. (1997)
R11r		$k_{11r} = k_{11f} / [2.7e-27 \exp(11,000/T)]$	Sander et al. (2006)
R9a	$\text{Cl}^-(aq) + \text{N}_2\text{O}_5 + \text{H}_2\text{O} \xrightarrow[\gamma_{\text{N}_2\text{O}_5}]{k_{9a}} \Phi \text{ClNO}_2 + (2-\Phi)\text{HNO}_3$	$k_{9a} = (\gamma_{\text{N}_2\text{O}_5} \omega_{\text{N}_2\text{O}_5} \text{SA})/4$	Model derived
R9b	$\text{Cl}^-(aq) + \text{ClNO}_2 + \text{H}_2\text{O} \xrightarrow[\gamma(\text{ClNO}_2)]{k_{9b}} \text{Cl}_2 + \text{HONO}$	$k_{9b} = (\gamma_{\text{ClNO}_2} \omega_{\text{ClNO}_2} \text{SA})/4$	Model derived

Note: SA is defined as wet aerosol surface area concentration (m^2/m^3), ω as mean thermal velocity (m/s), Φ as the yield of a reaction, and γ as the reaction probability of a reaction. Values of k_0 , k_∞ , and F can be found in the given reference.

formed during the time since sunset. The reaction probability of N_2O_5 , $\gamma(\text{N}_2\text{O}_5)$ is then adjusted until the modeled concentrations matched the observation of N_2O_5 for the wet aerosol surface area observed at the time of intercept. The yield of ClNO_2 , Φ (ClNO_2), from R9a is then adjusted until modeled concentrations of ClNO_2 match observations, after which, the total nitrate deposition velocity is adjusted until the initial concentration of total nitrate ($^T\text{NO}_3 = \text{HNO}_3 + \text{pNO}_3^-$ ($D_p < 4.1 \mu\text{m}$)) matches its concentration at the point of observation. Finally, γ (ClNO_2) is iteratively adjusted with extremely small changes in Φ (ClNO_2) (e.g., typically < 0.01) until Cl_2 and ClNO_2 concentrations predicted by the model match the observations within 5% of $[\text{Cl}_2]$. Figure 3 shows a collection of all 18 of the box model runs performed and the WINTER observations at the time since the previous 5pm local.

The inferred values for γ (ClNO_2) reported here are not strongly dependent upon $\gamma(\text{N}_2\text{O}_5)$, Φ (ClNO_2), or the deposition velocity of $^T\text{NO}_3$, used to match the observed concentrations of ClNO_2 , N_2O_5 , and $^T\text{NO}_3$, nor are they sensitive to other loss mechanisms of nitrate radical (NO_3) that are not included in this simple model (see Section 3.2). By using the observed concentration of $[\text{ClNO}_2]$ at a given time since sunset, the inferred γ (ClNO_2) does not change as $\gamma(\text{N}_2\text{O}_5)$ or Φ (ClNO_2) are adjusted so long as the model accurately reproduces the observed $[\text{ClNO}_2]$. The values used for $\gamma(\text{N}_2\text{O}_5)$ and Φ (ClNO_2) in analysis are generally constrained in that they must range between 0 and 1 and should agree with independent estimates from other field-based studies (Bannan et al., 2015; Faxon et al., 2015; Mielke et al., 2011, 2013; McDuffie, Fibiger, Dubé, Lopez-Hilfiker, et al., 2018; McDuffie, Fibiger, Dubé, Lopez-Hilfiker, et al., 2018; Osthoff et al., 2008; Phillips et al., 2012; Riedel et al., 2012, 2013; Tham et al., 2014; Thornton et al., 2010). The range of values for $\gamma(\text{N}_2\text{O}_5)$ and Φ (ClNO_2) used in our box model are 0.002–0.02 and 0.2–0.6, respectively, and are in good agreement with the study of these quantities during the WINTER campaign by McDuffie, Fibiger, Dubé, Lopez-Hilfiker, et al. (2018), McDuffie, Fibiger, Dubé, Lopez-Hilfiker, et al. (2018). Values for γ (ClNO_2) obtained by our box model analysis are mainly a function of aerosol surface area, temperature, concentrations of ClNO_2 and Cl_2 , time since sunset, and dilution, the sensitivities to all of which are discussed below in section 3.2.

3. 3. Results and Discussion

To match the observed Cl_2 concentrations from ClNO_2 uptake in all plumes, γ (ClNO_2) ranging from 6×10^{-6} to 7×10^{-5} , with a mean value of 2.3×10^{-5} ($\pm 1.8 \times 10^{-5}$) were required. Table 2 gives a summary of the derived values for γ (ClNO_2) for each of the plumes analyzed using the box model, a list of corresponding observations, and the correlation coefficient for each observation with the modeled γ (ClNO_2). Despite the ambient environment satisfying all the conditions at which Roberts et al. (2008) found conversion of ClNO_2 to Cl_2 to be 60–100% efficient, the values derived from the box model approach (γ (ClNO_2) $2.3 \times 10^{-5} \pm 1.8 \times 10^{-5}$) are at least 2 orders of magnitude below that reported on acidic laboratory films (γ (ClNO_2) = $6 \times 10^{-3} \pm 2 \times 10^{-3}$).

There are several possible reasons for the much slower conversion of ClNO_2 to Cl_2 in acidic ambient particles compared to that found in the laboratory. One possibility is that ClNO_2 is taken up into particles as quickly

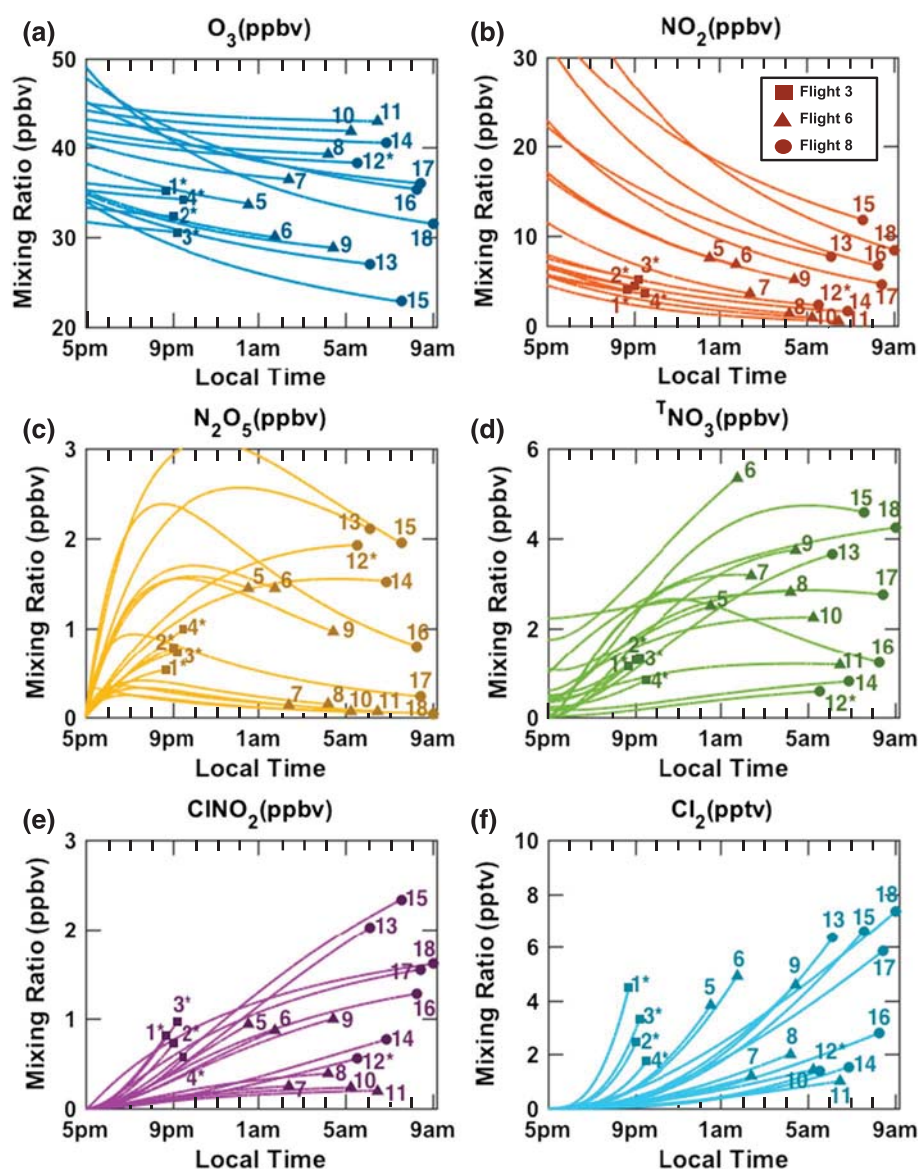


Figure 3. WINTER observations at the time of intercept (points) and the box model predictions (lines) for the concentrations of (a) O_3 , (b) NO_2 , (c) N_2O_5 , (d) TNO_3 , (e) ClNO_2 , and (f) Cl_2 and for each analyzed plume, noted with the referenced plume number.

as described in Roberts et al. (2008), but that the yield of reaction is significantly lower in atmospheric particles that contain reactants other than chloride. Our simulations inherently assume that the yield of (R9b) is unity, but competition of (R9b) with others that consume Cl^- (aq), like the formation of ClNO_2 , HCl , HOCl , or BrCl , would lower the yield of the reaction to form Cl_2 (Fickert et al., 1998; Frenzel et al., 1998). Our observations ultimately constrain the product of the γ (ClNO_2) and ϕ (Cl_2) from reaction (R9b). Figure 4 shows the range of γ (ClNO_2) that would be consistent with observations of ClNO_2 and Cl_2 by assuming different ϕ (Cl_2) < 1. In the median, if ClNO_2 uptake occurs as efficiently as found in Roberts et al. (2008), the observations require a yield of reaction (R9b) of 0.001, indicating only a small fraction of the absorbed ClNO_2 results in production of Cl_2 . Such a low ϕ (Cl_2) with high γ (ClNO_2) implies a large flux of pCl^- into different products. However, in four of the 18 plumes (plume #2, 3, 10, and 16), requiring such high uptake of ClNO_2 would simultaneously require a nonphysically large yield of ClNO_2 (i.e., ϕ (ClNO_2) > 1) in (R9a) to match the observed $[\text{ClNO}_2]$. Thus, our results imply that reactive uptake of

Table 2
Summary of Box Model Results and Corresponding Observations

Plume no.	Flight	γ_{ClNO_2}	pCl [−] ($\mu\text{g}/\text{m}^3$) ^a	D_p (μm) ^b	Time since sunset (hr) ^c	HCl (pptv)	[Cl [−]] (M) ^d	ClNO ₂ (pptv)	LWC ^e (M)	pOrg ^f ($\mu\text{g}/\text{m}^3$)	pNO ₃ ($\mu\text{g}/\text{m}^3$)	Cl ₂ (pptv)	Aerosol pH	SA ^g ($\mu\text{m}^2/\text{cm}^3$)	HOCl (pptv)	T (K)
1*	3	6.69×10^{-5}	0.137	0.47	3.72	1,352	0.20	812.6	30.5	2.05	1.27	4.47	1.45	227.3	9.3	273
2*	3	3.73×10^{-5}	0.112	0.47	4.07	861	0.16	724.5	28.4	2.02	1.47	2.46	1.48	269	7.3	273
3*	3	3.87×10^{-5}	0.083	0.48	4.22	952	0.12	967.3	30.9	2.15	1.73	3.31	1.38	273.8	6.9	273
4*	3	4.35×10^{-5}	0.085	0.42	4.53	712	0.18	565	27.3	1.51	0.83	1.75	1.53	212	5.2	274
5	6	1.74×10^{-5}	0.053	0.27	7.54	539	0.08	931.1	28.5	5.32	0.80	3.82	−0.15	412.9	8.3	274
6	6	1.67×10^{-5}	0.04	0.27	8.76	699	0.06	863	27.3	5.46	1.64	4.92	0.1	424.3	7.5	277
7	6	1.39×10^{-5}	0.02 [†]	0.29	9.44	583	0.03	248.2	40.2	2.12	0.07	1.18	−0.41	322	6.9	278
8	6	1.62×10^{-5}	0.03	0.26	11.20	623	0.06	387	35.6	1.83	0.04	2.01	−0.48	229	9.7	279
9	6	1.14×10^{-5}	0.03	0.28	11.43	517	0.04	994.9	31.6	3.31	0.30	4.58	−0.33	360.2	9.9	279
10	6	1.55×10^{-5}	0.043	0.29	12.25	574	0.09	232.2	40.2	1.40	0.01	1.44	−0.42	208.6	8.8	279
11	6	1.71×10^{-5}	0.07	0.23	13.48	348	0.35	196.6	36.5	1.31	0.03	1.01	−0.52	156.7	8.8	282
12*	8	1.60×10^{-5}	0.015 [†]	0.25	12.54	395	0.11	551.8	19.3	1.40	1.03	1.38	1.98	142	3.2	269
13	8	1.10×10^{-5}	0.028	0.17	13.17	433	0.10	2,022.9	18.5	3.76	3.45	6.35	1.96	275.9	8.5	270
14	8	1.22×10^{-5}	0.015 [†]	0.27	13.88	306	0.10	765.3	20.4	1.54	1.28	1.53	1.84	128.8	4.7	269
15	8	6.5×10^{-6}	0.02 [†]	0.18	14.58	465	0.05	2,336.4	17.2	3.19	3.80	6.59	2.0	317.2	6.9	270
16	8	8.3×10^{-6}	0.021 [†]	0.19	15.29	619	0.13	1,276.3	21.5	2.00	1.77	2.8	1.9	240.7	5.8	269
17	8	9.1×10^{-6}	0.02 [†]	0.2	15.50	770	0.09	1,546.6	18.4	2.35	2.42	5.86	1.39	213.5	6.4	270
18	8	8.1×10^{-6}	0.027	0.21	16.08	1,003	0.12	1,610	14.1	2.46	3.12	7.36	1.55	246.5	8.9	271
<i>r</i> with γ_{ClNO_2}			0.93 [‡]	0.89 [‡]	−0.86	0.70	0.44	−0.31	0.29	−0.21	−0.20	−0.18	0.14	−0.08	0.07	0.06

^aSum of Aerosol Mass Spectrometer (AMS) nonrefractory pCl[−] for $D_p^{\text{dry}} < 1 \mu\text{m} + 3\%$ UNH filter pCl[−] for $D_p^{\text{dry}} < 4 \mu\text{m}$. ^bWet particle diameter, derived from the calculated wet volume density to wet surface area density ratio. ^cTime of intercept of plume after 5 p.m., the “model sunset.” ^dCalculated chlorine molarity from measurements of a and b. ^eCalculated using ISORROPIA II following Haskins et al. (2018). ^fAMS measurements for $D_p^{\text{dry}} < 1 \mu\text{m}$. ^gCalculated wet surface area density from UHSAS measurements.

^{*}In all figures, asterisks denote plumes where wet aerosol surface area was estimated using the Aerosol Mass Spectrometer total mass. See text for details. [†]Denotes the AMS component of the pCl[−] measurement shown here was below detection limit ($0.024 \mu\text{g}/\text{m}^3$) and set to $1/2$ detection limit. [‡]Denotes statistical significance at the 95% level.

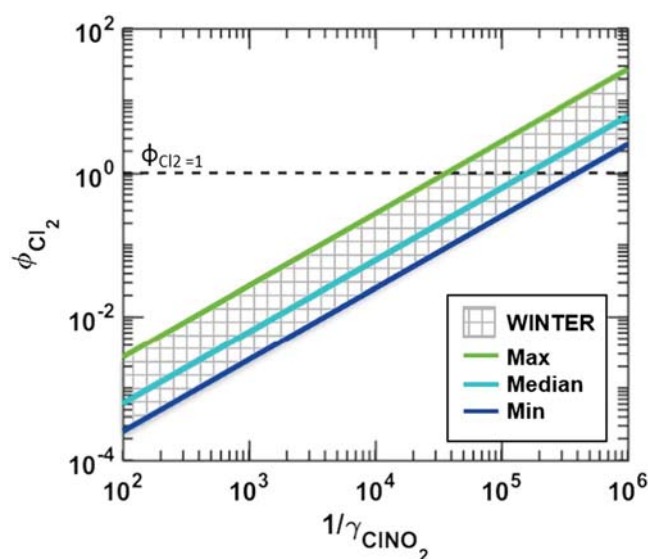


Figure 4. The range of WINTER constraints on the product of ϕ_{Cl_2} and γ_{ClNO_2} in all plumes. WINTER = Wintertime Investigation of Transport, Emissions, and Reactivity.

ClNO_2 as efficient as was observed in the laboratory cannot simultaneously explain all observations of ClNO_2 and Cl_2 during the WINTER campaign without invoking a major gap in our understanding of reactive chlorine chemistry.

A second possibility is that sufficient acidity to promote the reaction is not often collocated with available pCl^- . However, the ISORROPIA II calculations used in this work and examined in detail in Haskins et al., (2018), show that for the WINTER flights examined here submicron particles were predicted to have both $\text{pH} \leq 2$ and significant pCl^- and thus do not support this explanation. These ISORROPIA II calculations only examine bulk submicron aerosol pH under an assumption of internal mixing. Therefore, it is possible that particle pH is size dependent with submicron aerosols having lower pH, and supermicron aerosols having a higher concentration of pCl^- and a higher pH, perhaps higher than the $\text{pH} \leq 2$ threshold observed by Roberts et al. (2008), which would not be captured by this prediction of particle pH. This could imply that the formation of Cl_2 was occurring efficiently only on a fraction of the particles instead of inefficiently on all of them, as we find.

If we assume that production of Cl_2 takes place on only a fraction of the coarse mode aerosol population ($D_p > 1\text{--}3\mu\text{m}$) where most of the mass of chloride is expected and further assume that these particles are acidic

enough to promote the formation of Cl_2 , the required γ (ClNO_2) are on the order of 1×10^{-4} , which is not large enough to explain the discrepancy with laboratory results. We argue that internally mixed pCl^- in fact must exist in the submicron mode, as assuming that pCl^- only exists in the coarse mode implies both the production of ClNO_2 and subsequent uptake to form Cl_2 only occurs in the coarse mode. Under this situation, we require unrealistic physical values for $\gamma(\text{N}_2\text{O}_5)$ and ϕ (ClNO_2) in all plumes (e.g., ϕ (ClNO_2) > 1 , $\gamma(\text{N}_2\text{O}_5) > 0.1$) to reproduce the full suite of observations. Furthermore, HCl was observed in elevated concentrations during these three flights (Haskins et al., 2018), which is primarily formed via acid displacement at $\text{pH} 1\text{--}3$. In addition, the HNO_3 partitioning is highly sensitive to pH and the observed partitioning is consistent with the same thermodynamic models that predict pH [Guo et al., 2016; Haskins et al., 2018]. Thus, we conclude that the plumes examined in this work do simultaneously contain pCl^- and acidity sufficient to promote the reaction as observed in Roberts et al. (2008).

We have inherently assumed uptake occurs on all aerosols at the same rate, when it is possible that reactive uptake occurs with varying efficiency on particles of different sizes (e.g., submicron vs. super-micron particles), composition, and mixing state. However, without quantitative, size-resolved aerosol composition measurements across the size distribution, it is not possible to assess these issues beyond the sensitivity simulations presented in section 3.2, as our results represent an aerosol population-averaged value.

Given that a potential lack of colocated particle acidity and pCl^- seems unlikely to explain the discrepancy between field and laboratory derived γ (ClNO_2), we examined the relationship between the derived values for γ (ClNO_2) and other potential predictor variables, including pH, pCl^- mass concentration and Cl^- molarity, liquid water content, and volume-weighted mean wet particle diameter (wet D_p). We used a forward and backward linear stepwise regression model to add or remove the variables listed in Table 2, and weighted the observations that had estimated surface area densities from the AMS mass concentrations at half that of other observations due to larger uncertainties in the corresponding γ (ClNO_2). Parameters were added or removed from the model by determining if a p value for an F test of the change in the sum of squared error for the model was significant or not at the 95% level.

We found a rather simple result that wet D_p , and submicron pCl^- mass concentration, could explain 90% of the observed variance in the model derived γ (ClNO_2), within the 99% confidence level. In order to make the ISORROPIA II predicted chlorine partitioning consistent with measurements, Haskins et al., 2018 assumed a small fraction of refractory sea salt was present in particles with $D_p < 1\mu\text{m}$, amounting to $\sim 3\%$ of UNH (University of New Hampshire) filter chloride in the median during WINTER. Therefore, the pCl^-

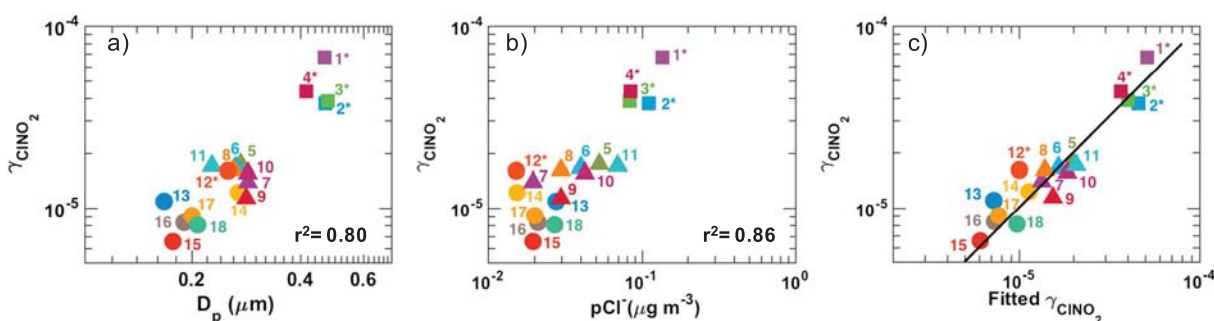


Figure 5. Scatter plots on a log scale of (a) the box model-derived γ (ClNO_2) and wet D_p and (b) the box model-derived γ (ClNO_2) and measured pCl^- (AMS + 3% filter), which are used in (c) the multilinear fit (x axis) of the box model-derived γ (ClNO_2) (y axis), assuming the yield of Cl_2 is 1.

measurement used in this work is the sum of the AMS nonrefractory chloride for dry $D_p < 1 \mu\text{m}$ and 3% of the UNH filter chloride for dry $D_p < 4.1 \mu\text{m}$. Values of AMS pCl^- lower than the detection limit ($0.024 \mu\text{g}/\text{m}^3$) were set to $1/2$ of the detection limit. The variations in the AMS nonrefractory chloride alone are enough to make pCl^- a significant predictor variable, while adding some refractory chloride from sea salt does statistically significantly improve the fit. D_p and pCl^- are not expected to be independent variables, but using them together provided a statistically significant change in the linear model's ability to predict the required γ (ClNO_2). The stepwise linear regression function that provided the best fit was γ (ClNO_2) = $6.67 \times 10^{-5} D_p + 2.22 \times 10^{-4} \text{pCl}^- - 1.0 \times 10^{-5}$ where D_p is in μm and pCl^- is in microgram per cubic meter, and should be considered valid only over the range of $D_p < 0.6 \mu\text{m}$ and $\text{pCl}^- < 0.2 \mu\text{g}/\text{m}^3$. It should be noted that the values of D_p and pCl^- used to calculate this empirical parameterization are not direct measurements of these values in the atmosphere but rely on estimates of aerosol growth factors and an equilibrium partitioning based estimate of refractory chloride contributions to submicron pCl^- . The validity of this empirical parameterization beyond conditions sampled during the WINTER campaign remains to be determined.

Figure 5 shows the variance of γ (ClNO_2) with wet D_p and pCl^- , and the multilinear fit estimated using the forward and backward linear stepwise regression model. The dependence on pCl^- availability of γ (ClNO_2) is reasonable as several processes compete to volatilize pCl^- into the gas phase in acidic aerosols. As such, the collocation of sufficient acidity to promote the reaction and available chloride may generally limit the production of Cl_2 from this mechanism, even if particles are not completely depleted in chloride. The trend in increasing γ (ClNO_2) with wet D_p is an indicator of a potentially volume-limited aqueous phase reaction, where the reaction rate in the particle phase is slow compared to diffusion, which has the form of equation ((1)):

$$\frac{1}{\gamma} = \frac{1}{\alpha} + \frac{3\omega}{4HRT R_p k_{\text{aq}}^I} \quad (1)$$

where α is the mass accommodation coefficient, ω is mean thermal speed (m/s), H is the Henry's law constant (M/atm), R is the gas constant ($\text{L}\cdot\text{atm}\cdot\text{mol}^{-1}\cdot\text{K}^{-1}$), T is temperature (K), R_p is particle radius (m), and k_{aq}^I is the first-order reaction rate (s^{-1}).

Several trends of note were observed in the other predictor variables listed in Table 2. Like the positive correlation with pCl^- , a positive correlation was found with HCl. HCl can serve as a reservoir of pCl^- via reversible equilibrium partitioning, such that in the presence of high HCl and higher pH, pCl^- could be replenished if this process could be competitive with the equilibrium partitioning of chloride to the gas phase under such acidic conditions. No statistically significant correlation was found with submicron aerosol pH, or liquid water content, presumably because the bulk calculated $\text{pH} < 2$ in all plumes and because particles were likely at least partially deliquesced in the humid marine boundary layer, such that acidity or presence of an aqueous phase was not a limiting factor in Cl_2 production..

A slight negative correlation, though not statistically significant, was found between γ (ClNO_2) and both submicron particle nitrate (pNO_3^-) and organic content (pOA), (both known to suppress absolute ClNO_2

formation via N_2O_5 uptake suppression) and likely to impact ClNO_2 uptake directly or indirectly (Bertram & Thornton, 2009; McDuffie, Fibiger, Dubé, Lopez-Hilfiker, et al., 2018; McDuffie, Fibiger, Dubé, Lopez Hilfiker, et al., 2018; Ryder et al., 2015). There was a distinct negative correlation between the required γ (ClNO_2) and the time after sunset at which the observations were made. It is possible this is due to a sampling bias in our measurements as the four plumes with the highest γ (ClNO_2) are those intercepted earliest in the night, where surface area was estimated with the total AMS mass and uncertainty is high. However, we cannot rule out that it could arise from a mechanism that either promotes uptake early in the evening, such as near source emissions, or a mechanism that suppresses uptake later in the night, such as chloride availability after particle processing.

Given the above finding that volume-weighted wet D_p is a strong predictor of the γ (ClNO_2), we hypothesize that the ClNO_2 reacto-diffusive length (ℓ), a measure of the characteristic distance an accommodated molecule must travel before reaction (Hanson et al., 1994), is larger than the mean D_p of sufficiently acidic aerosol particles sampled during WINTER. This hypothesis provides an explanation of the much lower γ (ClNO_2) derived from ambient measurements compared to those measured in the laboratory. In small atmospheric particles, ClNO_2 could be accommodated but diffuse out before reacting with pCl^- to form Cl_2 , thereby leading to a lower net γ (ClNO_2) in smaller aerosol particles than on the thicker laboratory films, which had aqueous volumes with effective thicknesses greater than hundreds of microns (Roberts et al., 2009).

To test this hypothesis, we estimate ℓ by extracting an observationally derived estimate for k_{aq}^I using equation (1) and the box model derived values for γ (ClNO_2), and subsequently solving for ℓ in equation (2) by assuming a liquid diffusion coefficient (D_l) of $1 \times 10^{-5} \text{ cm}^2/\text{s}$ (Cussler, 2009; Poling et al., 2001).

$$\ell = \left(\frac{D_l}{k_{\text{aq}}^I} \right)^{1/2} \quad (2)$$

Using the observed wet particle radius, R_p , temperature, a Henry's law constant of $4.6 \times 10^{-2} \text{ M/atm}$ (Frenzel et al., 1998), and assuming that $\alpha \gg \gamma$ (ClNO_2), over all plumes, we require a mean k_{aq}^I of $3.7 \times 10^4 \text{ s}^{-1} \pm 3.5 \times 10^4 \text{ s}^{-1}$ and ℓ of $0.2 \pm 0.05 \text{ }\mu\text{m}$ to match the box model-derived values of γ (ClNO_2).

With ℓ on the same order of magnitude as those observed wet D_p , and k_{aq}^I competitive with the liquid phase diffusion rate, these values imply that some fraction of accommodated ClNO_2 diffuses out of aerosol particles before reaction. This result explains why observationally constrained values of the γ (ClNO_2) are orders of magnitude lower than their estimated values on thick ($\sim 375 \text{ }\mu\text{m}$) laboratory films. Figure 6a shows the minimum, median, and maximum values for γ (ClNO_2) calculated from k_{aq}^I as a function of wet D_p compared to the box model derived values of γ (ClNO_2) at the observed wet D_p . The box model-derived γ (ClNO_2) exhibit a similar trend with D_p as that expected from equation (2) for a volume-limited process having ℓ on the order of $0.2 \text{ }\mu\text{m}$. If ambient particles were more viscous than pure water, or contained organics slowing liquid phase diffusion such that D_l was lower than the assumed value, the estimated ℓ would decrease promoting a faster k_{aq}^I . However, the presence of elevated ClNO_2 concentrations, formed from reactive uptake of N_2O_5 to aerosol, indicates that the ambient aerosol population sampled within these plumes are not strongly impacted by diffusion limiting conditions, like viscous organic coatings. The assumed α will not impact the values presented here, since α would have to be on the order of 1×10^{-5} , uncharacteristically low for liquid aerosols containing salt, in order to significantly impact γ (ClNO_2).

Our observationally constrained values for k_{aq}^I of $3.7 \times 10^4 \text{ s}^{-1} \pm 3.5 \times 10^4 \text{ s}^{-1}$ are orders of magnitude lower than those reported in Roberts et al. (2008) ($k_{\text{aq}}^I = 1.6 \times 10^7 \text{ s}^{-1}$). To investigate if this difference arises from a fundamentally slower reaction in ambient aerosols or because of lower chloride molarity in ambient aerosols, we use the derived k_{aq}^I and measured $[\text{Cl}^-]$ to extract a second-order rate coefficient, $\left(k_{\text{aq}}^{II} \equiv \frac{k_{\text{aq}}^I}{[\text{Cl}^-]} \right)$. Notably, the experiments preformed in Roberts et al. (2008) were done at low chloride molarity to simulate atmospheric particle concentrations ($[\text{Cl}^-] = 0.05 \text{ M}$), and are comparable to the range estimated from the plumes examined here ($0.03 \text{ M} < [\text{Cl}^-] < 0.35 \text{ M}$). However, as shown in Figure 6b as the slope of the linear least squares regression line, we find a median k_{aq}^{II} of $5.7 \times 10^4 \text{ M}^{-1} \text{ s}^{-1}$. This value is considerably lower than that reported in Roberts et al. (2008), suggesting that the difference in chloride molarity is not enough to explain the difference in implied reaction rates between the field measurements ($k_{\text{aq}}^{II} = 5.7 \times 10^4 \text{ M}^{-1} \text{ s}^{-1}$)

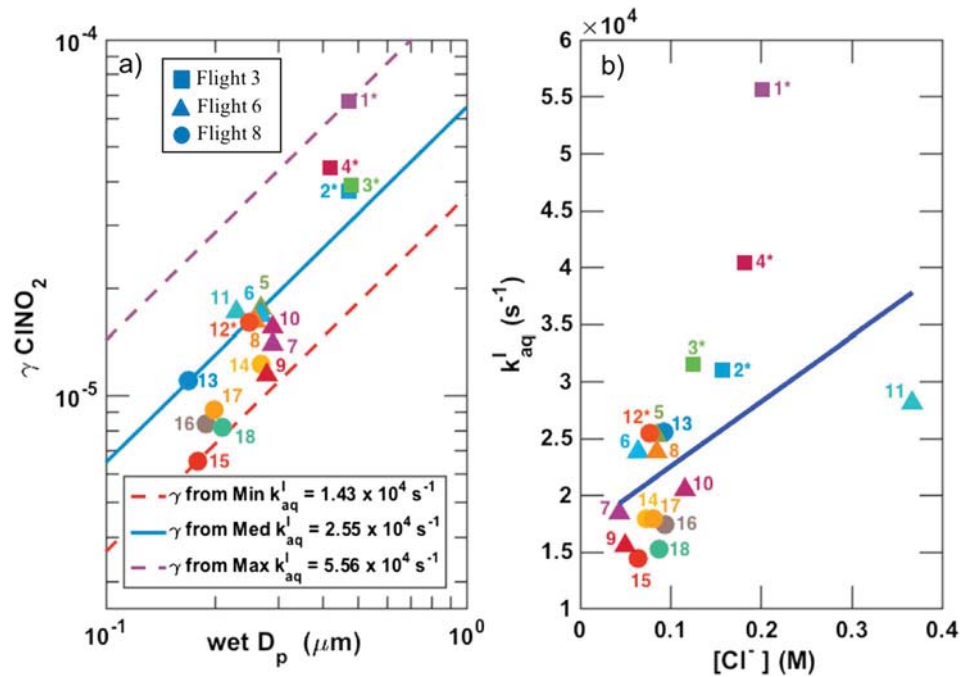


Figure 6. (a) The minimum, median, and maximum values for $\gamma(\text{ClNO}_2)$ calculated from the required k_{aq}^{I} as a function of wet D_p (lines) compared to the box model-derived values of $\gamma(\text{ClNO}_2)$ at the observed wet D_p (points). (b) Scatter plot of the first-order rate coefficients needed to match the box model-derived $\gamma(\text{ClNO}_2)$ versus the chloride molarity determined from the concentration of pCl^- (AMS + 3% filter) and UHSHS particle volume concentrations. The slope of the linear least squares fit (line), with plumes having estimated surface area (denoted with *) weighted at 50%, is the corresponding second-order rate coefficient.

and laboratory experiments ($k_{\text{aq}}^{\text{II}} \sim 10^7 \text{ M}^{-1} \text{ s}^{-1}$). Given that the $[\text{Cl}^-]$ used is an average over the aerosol size distribution calculated from three separate instruments data (AMS pCl^- , UNH pCl^- , UHSAS particle volume density), there is considerable uncertainty associated with this parameter, likely giving rise to deviations from the linear least squares regression fit shown in Figure 6b, though these uncertainties are unlikely to explain a 3 orders of magnitude difference in $k_{\text{aq}}^{\text{II}}$. Ultimately, our results suggest the reaction is fundamentally slower in small atmospheric particles ($D_p \sim 1 \mu\text{m}$) than inferred from thick ($\sim 375 \mu\text{m}$) laboratory films.

Hanson et al. (1994) derived the following expression to relate the effective uptake coefficient of a gas on small drops (γ_e) relative to its uptake coefficient on thick (approximately hundreds of micrometers) laboratory films (γ_m) as follows:

$$\frac{1}{\gamma_e} = \frac{1}{\alpha} + \frac{1}{\gamma_m [\coth(D_p/\ell) - \ell/D_p]} \quad (3)$$

where α is the mass accommodation coefficient. Assuming that $\alpha \gg \gamma$, equation (3) becomes:

$$\gamma_e \cong [\coth(D_p/\ell) - \ell/D_p] \gamma_m \quad (4)$$

In order to further test our hypothesis, we use equation (4), γ_m measured by Roberts et al. (2008), and the box model-derived values for γ_e with the measured D_p , to iteratively determine the implied ℓ and k_{aq}^{I} for each of the 18 plumes that would explain the difference in our model-derived $\gamma(\text{ClNO}_2)$ and the laboratory measured $\gamma(\text{ClNO}_2)$. Using this method, we estimated a mean ℓ on the order of $15 \mu\text{m}$ (compared to $0.2 \mu\text{m}$ using equation (2)) and values of k_{aq}^{I} considerably slower than our previous calculation. We attribute the discrepancy between our two methods of estimating ℓ to the uncertainty in the laboratory measured value, γ_m . The hyperbolic cotangent function in equation (4) is nonlinear, so small changes in γ_m result in orders of

magnitude changes in the estimated ℓ and k_{aq}^{-1} values. This result ultimately provides additional qualitative support for our hypothesis that the difference between our observationally constrained value of γ (ClNO₂) and those reported from laboratory measurements in Roberts et al. (2008) arise because R9b is volume-limited.

3.1. Model Sensitivity

Here we consider to what degree the inputs or assumptions used in the model may have influenced the field-derived reactive uptake coefficients. Several of the input uncertainties would lead to an overestimation in the box model-derived γ (ClNO₂) which is the opposite direction needed to explain the discrepancy between those observed in the laboratory and in our observations. We do not consider the possibility of direct emission of Cl₂ from anthropogenic point sources in any of the plumes analyzed here. While no plumes show clear evidence of being influenced by anthropogenic point sources of Cl₂, neglecting such a source would lead us to overestimate the γ (ClNO₂) needed to explain the observed Cl₂. Similarly, if the onset of N₂O₅ production were actually earlier than our assumed 5 p.m., we would also overestimate the γ (ClNO₂). The γ (ClNO₂) had to be decreased by ~8% if the sunset time was moved back an hour to 4 p.m.

We also reran the model setting sunset forward an hour to 6 p.m. After accounting for the changes in the initial concentrations of NO₂ and O₃ needed to match the observations at plume intercept, the yield of ClNO₂ from (R9a) had to be increased to match observations of ClNO₂, after which the γ (ClNO₂) had to be increased to match Cl₂ concentrations. For a typical plume, the γ (ClNO₂) had to be increased by ~10% if the sunset time was moved forward an hour, and for plume #1, γ (ClNO₂) increased by ~40%, resulting a maximum value of 9.5×10^{-5} , which implied a ℓ of 0.09 μm and k_{aq}^{-1} of $1.2 \times 10^5 \text{ s}^{-1}$, still consistent with the discrepancies between the field and laboratory studies resulting from a size-limited uptake coefficient. Moving the onset of N₂O₅ chemistry even later eventually leads to unrealistic values for γ (N₂O₅) and ϕ (ClNO₂).

Our 0-D model does not include NO₃ + VOC reactions, though these reactions would not significantly bias the results herein. Biogenic emissions, which often constitute the largest loss of NO₃, are greatly reduced in winter due to total lack of isoprene emissions and the strong temperature dependence of monoterpene emissions (Janson, 1993). Under WINTER conditions, McDuffie, Fibiger, Dubé, Lopez-Hilfiker, et al. (2018) calculated that the predicted equilibrium concentrations of NO₃ were typically more than 100 times lower than N₂O₅ and predicted only small fractional contributions of NO₃ to the total loss of NO₃ + N₂O₅. The box model approach employed in McDuffie, Fibiger, Dubé, Lopez-Hilfiker, et al. (2018), similar to that presented in our work, shows that despite the large number of uncertainties associated with direct NO₃ loss, 10% changes in total loss rates for NO₃ had a small impact on the box model predicted values of γ (N₂O₅). We expect the impact on the values of γ (ClNO₂) to be even smaller than that on γ (N₂O₅), because while including NO₃ + VOC reactions may slow N₂O₅ and ClNO₂ formation temporally, we only report instantaneous values of γ (ClNO₂), which are not dependent on the temporal evolution of N₂O₅ and ClNO₂, but their absolute concentrations, which we require the box model to reproduce at the time of intercept.

Another consideration is that Cl₂ may be produced from HOCl or ClONO₂ uptake, instead of from ClNO₂ uptake alone as we currently assume. Using γ (HOCl) from Lawler et al., (2011) during the low accommodation case to produce Cl₂, there is not enough HOCl present to explain the Cl₂ concentrations in 6 of the 18 plumes observed. Thus, it is impossible to completely rule out the conversion of HOCl to Cl₂ on surfaces, in all plumes analyzed here, but if it was occurring, it would bias our box model-derived γ (ClNO₂) values high, in which case, the true γ (ClNO₂) would be even lower, thereby increasing the observed discrepancy between the field and laboratory measurements. Measurements of ClONO₂ were not available during WINTER, so estimates of its contributions to observed Cl₂ concentrations cannot be made. However, Breton et al., (2018) report 15 pptv of ClONO₂ throughout the night in a polluted region of China. Under the conditions observed during WINTER, the relevant uptake coefficients, 4.6×10^{-3} to 0.14 (Burkholder et al., 2015) of ClONO₂, would predict complete conversion of 15 pptv of ClONO₂ into Cl₂ within 15 min to 6 hr, and the production of >40 pptv Cl₂ if such concentrations of ClONO₂ were sustained throughout the night, which is significantly higher than WINTER observations. Such a rapid turnover of ClONO₂ would imply a nighttime formation mechanism of ClONO₂, of which we have no knowledge. Thus, we conclude that ClONO₂ heterogeneous chemistry was not an important source of Cl₂ during WINTER, and to the extent it was

occurring, we would need to further slow ClNO₂ conversion to Cl₂, increasing the discrepancy between laboratory and field.

Due to large flight-by-flight uncertainties in dilution rates, dilution was not included in the initial box model analysis. Therefore, a sensitivity simulation was run where dilution was represented as an additional first-order loss process for all chemical species in the mechanism (Table 2). Following McDuffie, Fibiger, Dubé, Lopez-Hilfiker, et al. (2018), the dilution rate constant was set to a constant value of $3.1 \times 10^{-5} \text{ s}^{-1}$ as calculated from NO_y mixing ratio changes in a single air parcel measured at multiple times during RF03. For all species except O₃, concentrations in background air outside plumes was set to zero. Background levels of O₃ were calculated on a flight-by-flight basis as the intercept of the O₃/NO_y correlation plot. Considering dilution increased $\gamma(\text{ClNO}_2)$ by only 5% in the median, requiring a maximum $\gamma(\text{ClNO}_2)$ of 6.8×10^{-5} , which does not significantly change the results presented herein.

Uncertainty in the calculated aerosol growth factors can affect the available surface area for heterogeneous chemistry. Instead of using a surface area concentration based on deliquesced particles, we reran the model using the aerosol dry surface area. At most, $\gamma(\text{ClNO}_2)$ had to be increased by 30 to 60%. Even together with the maximum uncertainty in the time for onset of N₂O₅ production and dilution used in the model, this was not enough to significantly impact the results presented here. Therefore, we conclude that the uncertainties in our model inputs are not enough to explain the discrepancy in the observationally constrained values and laboratory measurements of $\gamma(\text{ClNO}_2)$ and that the strong correlations between model-derived $\gamma(\text{ClNO}_2)$, particle size, and pCl[−] suggest that this chemistry may be size and chloride limited in the atmosphere, thereby serving to reduce the production efficiency of Cl₂ compared to that inferred from laboratory studies on macroscopic films.

4. 4. Conclusions

We have presented simultaneous observations of Cl₂ and ClNO₂ in 18 highly correlated plumes from the WINTER campaign where in situ production of Cl₂ is more likely than direct emission. Using a simple zero-dimensional box model to simulate the nocturnal chemical evolution of an air parcel, we derived values for $\gamma(\text{ClNO}_2)$ required to explain observed Cl₂ from ClNO₂ uptake ranging from 6.5×10^{-6} to 6.7×10^{-5} , with a mean value of 2.3×10^{-5} ($\pm 1.8 \times 10^5$). These uptake coefficients are 2 orders of magnitude lower than previous laboratory observations on acidic surfaces, despite independent indications that submicron particle pH was less than 2 and pCl[−] was nonzero, the conditions under which this reaction was seen to proceed with 60–100% efficiency (Roberts et al., 2008). Assuming ClNO₂ uptake as efficient as observed in the laboratory, but occurring with a very low yield of Cl₂ ($\phi(\text{Cl}_2) = 0.001$), we were unable to match the observed [ClNO₂] and [Cl₂] concentrations in 4 of the 18 plumes analyzed. We cannot rule out the simultaneous uptake of HOCl or ClONO₂ contributing to the observed Cl₂ concentrations, though these would bias our derived values for $\gamma(\text{ClNO}_2)$ high, the opposite direction needed for agreement with laboratory values.

We found a strong dependence of the observationally constrained values for $\gamma(\text{ClNO}_2)$ on both pCl[−] and volume-weighted wet D_p , indicating that the efficiency with which ClNO₂ is converted to Cl₂ is both dependent on the availability of collocated pCl[−] and sufficient acidity to promote the reaction, and that $\gamma(\text{ClNO}_2)$ is volume limited. We hypothesize the most plausible explanation for the discrepancy in our field-derived $\gamma(\text{ClNO}_2)$ and those measured in the laboratory stems from the different length scales in macroscopic films or salt beds used in the laboratory compared to submicron particles. We estimate that the first-order reaction rate constant in the 18 plumes examined here is k_{aq}^{I} of $3.7 \times 10^4 \text{ s}^{-1} \pm 3.5 \times 10^4 \text{ s}^{-1}$, which implies a second-order reaction rate constant of $k_{\text{aq}}^{\text{II}} = 5.7 \times 10^4 \text{ M}^{-1} \text{ s}^{-1}$ using the observationally constrained chloride molarity.

Ultimately, our work suggests a need for direct laboratory studies of ClNO₂ reactive uptake on acidic submicron aerosol particles. It is possible that our inference of a size dependence is rather a result of some other limitation not considered here, such as an equilibrium between particle chloride, nitrite, Cl₂ and ClNO₂. A laboratory experiment using acidic submicron particles would directly test these hypotheses. At this time, our observations suggest models use a much lower $\gamma(\text{ClNO}_2)$ on the order of 2.3×10^{-5} ($\pm 1.8 \times 10^5$), to simulate Cl₂ production on acidic aerosols from nocturnal reactive nitrogen chemistry.

Acknowledgments

This work was supported by the National Science Foundation (NSF) under Grant AGS-1360745 to J. A. T. as part of the WINTER aircraft campaign with support from the National Oceanic and Atmospheric Administration's Earth System Research Laboratory. Additionally, we acknowledge support for this work from the NSF under Grant AGS-1822664 to J. L. J. The WINTER data are provided by NCAR/EOL under sponsorship of the NSF (<http://data.eol.ucar.edu>).

References

- Bannan, T. J., Booth, A. M., Bacak, A., Muller, J. B. A., Leather, K. E., Le Breton, M., et al. (2015). The first UK measurements of nitryl chloride using a chemical ionization mass spectrometer in central London in the summer of 2012, and an investigation of the role of Cl atom oxidation. *Journal of Geophysical Research: Atmospheres*, 120, 1–20. <https://doi.org/10.1002/2014JD022629>
- Behnke, W., George, C., Scheer, V., & Zetzsch, C. (1997). Production and decay of ClNO₂ from the reaction of gaseous N₂O₅ with NaCl solution: Bulk and aerosol experiments. *Journal of Geophysical Research*, 102, 3795–3804.
- Bertram, T. H., & Thornton, J. A. (2009). Toward a general parameterization of N₂O₅ reactivity on aqueous particles: the competing effects of particle liquid water, nitrate and chloride. *Atmospheric Chemistry and Physics*, 9, 8351–8363. <https://doi.org/10.5194/acp-9-8351-2009>
- Brown, S. S., Stark, H., & Ravishankara, A. R. (2003). Applicability of the steady state approximation to the interpretation of atmospheric observations of NO₃ and N₂O₅. *Journal of Geophysical Research*, 108(D17), 4539. <https://doi.org/10.1029/2003JD003407>
- Burkholder, J. B., Sander, S. P., Abbatt, J. P. D., Barker, J. R., Huie, R. E., Kolb, C. E., et al. (2015). *Chemical kinetics and photochemical data for use in atmospheric studies: Evaluation number 18*. Pasadena, CA: Jet Propulsion Laboratory, National Aeronautics and Space Administration.
- Cussler, E. L. (2009). *Diffusion: Mass transfer in fluid systems* (3rd ed.). Cambridge, UK: Cambridge University Press.
- Custard, K. D., Raso, A. R. W., Shepson, P. B., Staebler, R. M., & Pratt, K. A. (2017). Production and release of molecular bromine and chlorine from the Arctic coastal snowpack. *ACS Earth and Space Chemistry*, 1(3), 142–151. <https://doi.org/10.1021/acsearthspacechem.7b00014>
- DeMore, W. B., Sander, S. P., Golden, D. M., Hampson, R. F., Kurylo, M. J., Howard, C. J., et al. (1997). *Chemical kinetics and photochemical data for use in stratospheric modeling: Eval. 12*. Pasadena, Calif: Jet Propul. Lab.
- Faxon, C., Bean, J., & Hildebrandt-Ruiz, L. (2015). Inland concentrations of ClNO₂ in Southeast Texas suggest chlorine chemistry significantly contributes to atmospheric reactivity. *Atmosphere*, 6 (Atmospheric Composition Observations), 1487–1506. <https://doi.org/10.3390/atmos6101487>
- Fibiger, D. L., McDuffie, E. E., Dubé, W. P., Aikin, K. C., Lopez-Hilfiker, F. D., Lee, B. H., et al. (2018). Wintertime overnight NO_x removal in a Southeastern United States coal-fired power plant plume: A model for understanding winter NO_x processing and its implications. *Journal of Geophysical Research: Atmospheres*, 123, 1412–1425. <https://doi.org/10.1002/2017JD027768>
- Fickert, S., Helleis, F., Adams, J. W., Moortgat, G. K., & Crowley, J. N. (1998). Reactive uptake of ClNO₂ on aqueous bromide solutions. *The Journal of Physical Chemistry. A*, 102, 10,689–10,696.
- Finlayson-Pitts, B., Ezell, M., & Pitts, J. (1989). Formation of chemically active chlorine compounds by reactions of atmospheric NaCl particles with gaseous N₂O₅ and ClONO₂. *Nature*, 337(6204), 241–244. <https://doi.org/10.1038/337241a0>
- Finley, B. D., & Saltzman, E. S. (2006). Measurement of Cl₂ in coastal urban air. *Geophysical Research Letters*, 33, L11809. <https://doi.org/10.1029/2006gl025799>
- Frenzel, A., Scheer, V., Sikorski, R., George, C., Behnke, W., & Zetzsch, C. (1998). Heterogeneous interconversion reactions of BrNO₂, ClNO₂, Br₂, and Cl₂. *The Journal of Physical Chemistry A*, 102(8), 1329–1337. <https://doi.org/10.1021/jp973044b>
- George, C., Behnke, W., Scheer, V., Zetzsch, C., Magi, L., Ponche, J. L., & Mirabel, P. (1995). Fate of ClNO₂ over aqueous solutions containing iodide. *Geophysical Research Letters*, 22, 1505–1508.
- Graedel, T. E., & Keene, W. C. (1995). Tropospheric budget of reactive chlorine. *Global Biogeochemical Cycles*, 9(1), 47–77. <https://doi.org/10.1029/94GB03103>
- Guo, H., Liu, J., Froyd, K. D., Roberts, J. M., Veres, P. R., Hayes, P. L., et al. (2017). Fine particle pH and gas-particle phase partitioning of inorganic species in Pasadena, California, during the 2010 CalNex campaign. *Atmospheric Chemistry and Physics*, 17, 5703–5719. <https://doi.org/10.5194/acp-17-5703-2017>
- Guo, H., Sullivan, A. P., Campuzano-Jost, P., Schroder, J. C., Lopez-Hilfiker, F. D., Dibb, J. E., et al. (2016). Fine particle pH and the partitioning of nitric acid during winter in the northeastern United States. *Journal of Geophysical Research: Atmospheres*, 121, 10,355–10,376. <https://doi.org/10.1002/2016JD025311>
- Guo, H., Xu, L., Bougiatioti, A., Cerully, K. M., Capps, S. L., Hite, J. R. Jr., et al. (2015). Fine-particle water and pH in the southeastern United States. *Atmospheric Chemistry and Physics*, 15(9), 5211–5228. <https://doi.org/10.5194/acp-15-5211-2015>
- Hanson, D. R., & Ravishankara, A. R. (1994). Reactive uptake of ClONO₂ onto sulfuric acid due to reaction with HCl and H₂O. *The Journal of Physical Chemistry*, 98(22), 5728–5735. <https://doi.org/10.1021/j100073a026>
- Hanson, D. R., Ravishankara, A. R., & Solomon, S. (1994). Heterogeneous reactions in sulfuric acid aerosols: A framework for model calculations. *Journal of Geophysical Research*, 99(D2), 3615–3629. <https://doi.org/10.1029/93JD02932>
- Haskins, J. D., Jaeglé, L., Shah, V., Lee, B. H., Lopez-Hilfiker, F. D., Campuzano-Jost, P., et al. (2018). Wintertime gas-particle partitioning and speciation of inorganic chlorine in the lower troposphere over the Northeast United States and coastal ocean. *Journal of Geophysical Research: Atmospheres*, 123. <https://doi.org/10.1029/2018JD028786>
- Jaeglé, L., Shah, V., Thornton, J. A., Lopez-Hilfiker, F. D., Lee, B. H., McDuffie, E. E., et al. (2018). Nitrogen oxides emissions, chemistry, deposition, and export over the Northeast United States during the WINTER aircraft campaign. *Journal of Geophysical Research: Atmospheres*, 123, 12,368–12,393. <https://doi.org/10.1029/2018JD029133>
- Janson, R. W. (1993). Monoterpene emissions from Scots pine and Norwegian spruce. *Journal of Geophysical Research*, 98(D2), 2839–2850. <https://doi.org/10.1029/92JD02394>
- Keene, W. C., Maben, J. R., Pszenny, A. A. P., & Galloway, J. N. (1993). Measurement technique for inorganic chlorine gases in the marine boundary layer. *Environmental Science & Technology*, 27, 866–874. <https://doi.org/10.1021/es00042a008>
- Keene, W. C., Stutz, J., Pszenny, A. A., Maben, J. R., Fischer, E. V., Smith, A. M., et al. (2007). Inorganic chlorine and bromine in coastal New England air during summer. *Journal of Geophysical Research*, 112, D10S12. <https://doi.org/10.1029/2006JD007689>
- Kenagy, H. S., Sparks, T. L., Ebben, C. J., Wooldridge, P. J., Lopez-Hilfiker, F. D., Lee, B. H., et al. (2018). NO_x lifetime and NO_y partitioning during WINTER. *Journal of Geophysical Research: Atmospheres*, 123, 9813–9827. <https://doi.org/10.1029/2018JD028736>
- Knipping, E. M., Lakin, M. J., Foster, K. L., Jungwirth, P., Tobias, D. J., Gerber, R. B., et al. (2000). Experiments and simulations of ion-enhanced interfacial chemistry on aqueous NaCl aerosols. *Science*, 288(5464), 301–306. <https://doi.org/10.1126/science.288.5464.301>
- Laskin, A., Moffet, R. C., Gilles, M. K., Fast, J. D., Zaveri, R. A., Wang, B., et al. (2012). Tropospheric chemistry of internally mixed sea salt and organic particles: Surprising reactivity of NaCl with weak organic acids. *Journal of Geophysical Research*, 117, D15302. <https://doi.org/10.1029/2012JD017743>
- Lawler, M. J., Sander, R., Carpenter, L. J., Lee, J. D., Von Glasow, R., Sommariva, R., & Saltzman, E. S. (2011). HOCl and Cl₂ observations in marine air. *Atmospheric Chemistry and Physics*, 11(15), 7617–7628. <https://doi.org/10.5194/acp-11-7617-2011>

- Lee, B. H., Lopez-Hilfiker, F. D., Schroder, J. C., Campuzano-Jost, P., Jimenez, J. L., McDuffie, E. E., et al. (2018). Airborne observations of reactive inorganic chlorine and bromine species in the exhaust of coal-fired power plants. *Journal of Geophysical Research: Atmospheres*, 123(19), 11,211–225,237. <https://doi.org/10.1029/2018JD029284>
- Lee, B. H., Lopez-Hilfiker, F. D., Veres, P. R., McDuffie, E. E., Fibiger, D. L., Sparks, T. L., et al. (2018). Flight deployment of a high-resolution time-of-flight chemical ionization mass spectrometer: Observations of reactive halogen and nitrogen oxide species. *Journal of Geophysical Research: Atmospheres*, 123(14), 7670–7686. <https://doi.org/10.1029/2017JD028082>
- Liao, J., Huey, L. G., Liu, Z., Tanner, D. J., Cantrell, C. A., Orlando, J. J., et al. (2014). High levels of molecular chlorine in the Arctic atmosphere. *Nature Geoscience*, 7, 91. <https://doi.org/10.1038/ngeo2046>
- Liu, X., Qu, H., Huey, L. G., Wang, Y., Sjostedt, S., Zeng, L., et al. (2017). High levels of daytime molecular chlorine and nitryl chloride at a rural site on the North China Plain. *Environmental Science & Technology*, 51(17), 9588–9595. <https://doi.org/10.1021/acs.est.7b03039>
- Liu, Y., Fan, Q., Chen, X., Zhao, J., Ling, Z., Hong, Y., et al. (2018). Modeling the impact of chlorine emissions from coal combustion and prescribed waste incineration on tropospheric ozone formation in China. *Atmospheric Chemistry and Physics*, 18, 2709–2724. <https://doi.org/10.5194/acp-18-2709-2018>
- McDuffie, E. E., Fibiger, D. L., Dubé, W. P., Lopez-Hilfiker, F., Lee, B. H., Jaeglé, L., et al. (2018). ClNO₂ Yields from aircraft measurements during the 2015 WINTER campaign and critical evaluation of the current parameterization. *Journal of Geophysical Research: Atmospheres*, 123(22), 12,15,913–12,15,994. <https://doi.org/10.1029/2018JD029358>
- McDuffie, E. E., Fibiger, D. L., Dubé, W. P., Lopez-Hilfiker, F., Lee, B. H., Thornton, J. A., et al. (2018). Heterogeneous N₂O₅ uptake during winter: Aircraft measurements during the 2015 WINTER campaign and critical evaluation of current parameterizations. *Journal of Geophysical Research: Atmospheres*, 123, 4345–4372. <https://doi.org/10.1002/2018JD028336>
- Mielke, L. H., Furgeson, A., & Osthoff, H. D. (2011). S.I.: Observation of ClNO in a mid-continental urban environment. *Environmental Science & Technology*, 45, 8889–8896. <https://doi.org/10.1021/es201955u>
- Osthoff, H. D., Roberts, J. M., Ravishankara, A. R., Williams, E. J., Lerner, B. M., Sommariva, R., et al. (2008). High levels of nitryl chloride in the polluted subtropical marine boundary layer. *Nature Geoscience*, 1(5), 324–328. <https://doi.org/10.1038/ngeo177>
- Pechtl, S., & von Glasow, R. (2007). Reactive chlorine in the marine boundary layer in the outflow of polluted continental air: A model study. *Geophysical Research Letters*, 34, L11813. <https://doi.org/10.1029/2007GL029761>
- Phillips, G. J., Tang, M. J., Thieser, J., Brickwedde, B., Schuster, G., Bohn, B., et al. (2012). Significant concentrations of nitryl chloride observed in rural continental Europe associated with the influence of sea salt chloride and anthropogenic emissions. *Geophysical Research Letters*, 39, L10811. <https://doi.org/10.1029/2012GL051912>
- Phillips, G. J., Thieser, J., Tang, M., Sobanski, N., Schuster, G., Fachinger, J., et al. (2016). Estimating N₂O₅ uptake coefficients using ambient measurements of NO₃, N₂O₅, ClNO₂ and particle-phase nitrate. *Atmospheric Chemistry and Physics*, 16, 13,231–13,249. <https://doi.org/10.5194/acp-16-13231-2016>
- Poling, B. E., Prausnitz, J. M., & O'Connell, J. P. (2001). *The properties of gases and liquids* (Vol. 5). New York: McGraw-Hill.
- Pratt, K. A., Custard, K. D., Shepson, P. B., Douglas, T., Pöhler, D., General, S., et al. (2013). Photochemical production of molecular bromine in Arctic surface snowpacks. *Nature Geoscience*, 6(5), 351–356.
- Pszeny, A. A. P., Keene, W. C., Jacob, D. J., Fan, S., Maben, J. R., Zetwo, M. P., et al. (1993). Evidence of inorganic chlorine gases other than hydrogen chloride in marine surface air. *Geophysical Research Letters*, 20(8), 699–702. <https://doi.org/10.1029/93gl00047>
- Pszeny, A. A. P., Moldanová, J., Keene, W. C., Sander, R., Maben, J. R., Martinez, M., et al. (2004). Halogen cycling and aerosol pH in the Hawaiian marine boundary layer. *Atmospheric Chemistry and Physics*, 4(1), 147–168. Retrieved from <https://hal.archives-ouvertes.fr/hal-00295390>
- Ren, X., Salmon, O. E., Hansford, J. R., Ahn, D., Hall, D., Benish, S. E., et al. (2018). Methane emissions from the Baltimore-Washington area based on airborne observations: Comparison to emissions inventories. *Journal of Geophysical Research: Atmospheres*, 123, 8869–8882. <https://doi.org/10.1029/2018JD028851>
- Riedel, T. P., Bertram, T. H., Crisp, T. A., Williams, E. J., Lerner, B. M., Vlasenko, A., et al. (2012). Nitryl chloride and molecular chlorine in the coastal marine boundary layer. *Environmental Science and Technology*. <https://doi.org/10.1021/es204632r>
- Riedel, T. P., Wagner, N. L., Dubé, W. P., Middlebrook, A. M., Young, C. J., Öztürk, F., et al. (2013). Chlorine activation within urban or power plant plumes: Vertically resolved ClNO₂ and Cl₂ measurements from a tall tower in a polluted continental setting. *Journal of Geophysical Research: Atmospheres*, 118, 8702–8715. <https://doi.org/10.1002/jgrd.50637>
- Riedel, T. P., Wolfe, G. M., Danas, K. T., Gilman, J. B., Kuster, W. C., Bon, D. M., et al. (2014). An MCM modeling study of nitryl chloride (ClNO₂) impacts on oxidation, ozone production and nitrogen oxide partitioning in polluted continental outflow. *Atmospheric Chemistry and Physics*, 14(8), 3789–3800. <https://doi.org/10.5194/acp-14-3789-2014>
- Roberts, J. M., Osthoff, H. D., Brown, S. S., & Ravishankara, A. R. (2008). N₂O₅ Oxidizes Chloride to Cl₂ in Acidic Atmospheric Aerosol. *Science*, 321(5892), 1059.
- Roberts, J. M., Osthoff, H. D., Brown, S. S., Ravishankara, A. R., Coffman, D., Quinn, P., & Bates, T. (2009). Laboratory studies of products of N₂O₅ uptake on Cl⁻ containing substrates. *Geophysical Research Letters*, 36, L20808. <https://doi.org/10.1029/2009GL040448>
- Ryder, O. S., Campbell, N. R., Shaloski, M., Al-Mashat, H., Nathanson, G. M., & Bertram, T. H. (2015). Role of organics in regulating ClNO₂ production at the air-sea interface. *The Journal of Physical Chemistry A*, 119(31), 8519–8526. <https://doi.org/10.1021/jp5129673>
- Saiz-Lopez, A., & von Glasow, R. (2012). Reactive halogen chemistry in the troposphere. *Chemical Society Reviews*, 41(19), 6448–6472. <https://doi.org/10.1039/C2CS35208G>
- Salmon, O. E., Shepson, P. B., Ren, X., He, H., Hall, D. L., Dickerson, R. R., et al. (2018). Top-down estimates of NO_x and CO emissions from Washington, D.C.-Baltimore during the WINTER campaign. *Journal of Geophysical Research: Atmospheres*, 123, 7705–7724. <https://doi.org/10.1029/2018JD028539>
- Salmon, O. E., Shepson, P. B., Ren, X., Marquardt Collow, A. B., Miller, M. A., Carlton, A. G., et al. (2017). Urban emissions of water vapor in winter. *Journal of Geophysical Research: Atmospheres*, 122, 9467–9484. <https://doi.org/10.1002/2016JD026074>
- Sander, S. P., Finlayson-Pitts, B. J., Friedl, R. R., Golden, D. M., Huie, R. E., Kolb, C. E., et al. (2003). *Chemical kinetics and photochemical data for use in atmospheric studies, Evaluation Number 14*. Pasadena, CA: JPL Publication 02-25, Jet Propulsion Laboratory.
- Sander, S. P., Golden, D. M., Kurylo, M. J., Moortgat, G. K., Wine, P. H., Ravishankara, A. R., et al. (2006). *Chemical kinetics and photochemical data for use in atmospheric studies, Evaluation Number 15*. Pasadena, CA: JPL Publication 07-10, Jet Propulsion Laboratory.
- Schmidt, J. A., Jacob, D. J., Horowitz, H. M., Hu, L., Sherwen, T., Evans, M. J., et al. (2016). Modeling the observed tropospheric BrO background: Importance of multiphase chemistry and implications for ozone, OH, and mercury. *Journal of Geophysical Research: Atmospheres*, 121, 11,811–11,819, 835. <https://doi.org/10.1002/2015JD024229>

- Schroder, J. C., Campuzano-Jost, P., Day, D. A., Shah, V., Larson, K., Sommers, J. M., et al. (2018). Sources and secondary production of organic aerosols in the northeastern United States during WINTER. *Journal of Geophysical Research: Atmospheres*, 123, 7771–7796. <https://doi.org/10.1029/2018JD028475>
- Schweitzer, F., Mirabel, P., & George, C. (1998). Multiphase chemistry of N₂O₅, ClNO₂ and BrNO₂. *The Journal of Physical Chemistry. A*, 102, 3942–3952.
- Shah, V., Jaeglé, L., Thornton, J. A., Lopez-Hilfiker, F. D., Lee, B. H., Schroder, J. C., et al. (2018). Chemical feedbacks weaken the wintertime response of particulate sulfate and nitrate to emissions reductions over the eastern United States. *Proceedings of the National Academy of Sciences*, 115(32), 8110 LP–8115. <https://doi.org/10.1073/pnas.1803295115>
- Sherwen, T., Schmidt, J. A., Evans, M. J., Carpenter, L. J., Großmann, K., Eastham, S. D., et al. (2016). Global impacts of tropospheric halogens (Cl, Br, I) on oxidants and composition in GEOS-Chem. *Atmospheric Chemistry and Physics*, 16, 12,239–12,271. <https://doi.org/10.5194/acp-16-12239-2016>
- Simpson, W. R., Brown, S. S., Saiz-Lopez, A., Thornton, J. A., & Von Glasow, R. (2015). Tropospheric halogen chemistry: Sources, cycling, and impacts. *Chemical Reviews*, 115(10), 4035–4062. <https://doi.org/10.1021/cr5006638>
- Spicer, C. W., Chapman, E. G., Finlayson-Pitts, B. J., Plastridge, R. A., Hubbe, J. M., Fast, J. D., & Berkowitz, C. M. (1998). Unexpectedly high concentrations of molecular chlorine in coastal air. *Nature*, 394(6691), 353–356. <https://doi.org/10.1038/28584>
- Sullivan, A. P., Guo, H., Schroder, J. C., Campuzano-Jost, P., Jimenez, J. L., Campos, T., Shah, V., Jaeglé, L., Lee, B. H., Lopez-Hilfiker, F. D., Thornton, J. A., Brown, S. S., Weber, R. J. (2019). Biomass burning markers and residential burning in the WINTER aircraft campaign. *Journal of Geophysical Research: Atmospheres*, 124, 1846–1861. <https://doi.org/10.1029/2017JD028153>
- Tanaka, P. L., Oldfield, S., Neece, J. D., Mullins, C. B., & Allen, D. T. (2000). Anthropogenic sources of chlorine and ozone formation in urban atmospheres. *Environmental Science & Technology*, 34(21), 4470–4473. <https://doi.org/10.1021/es991380v>
- Tham, Y. J., Wang, Z., Li, Q., Wang, W., Wang, X., Lu, K., et al. (2018). Heterogeneous N₂O₅ uptake coefficient and production yield of ClNO₂ in polluted northern China: Roles of aerosol water content and chemical composition. *Atmospheric Chemistry and Physics Discussions*. <https://doi.org/10.5194/acp-2018-313>
- Tham, Y. J., Yan, C., Xue, L., Zha, Q., Wang, X., & Wang, T. (2014). Presence of high nitryl chloride in Asian coastal environment and its impact on atmospheric photochemistry. *Chinese Science Bulletin*, 59(4), 356–359. <https://doi.org/10.1007/s11434-013-0063-y>
- Thornton, J. A., Kercher, J. P., Riedel, T. P., Wagner, N. L., Cozic, J., Holloway, J. S., et al. (2010). A large atomic chlorine source inferred from mid-continental reactive nitrogen chemistry. *Nature*, 464(7286), 271–274. <https://doi.org/10.1038/nature08905>
- Vogt, R., Crutzen, P. J., & Sander, R. (1996). A mechanism for halogen release from sea salt aerosol in the remote marine boundary layer. *Nature*, 383(6598), 327–330. <http://doi.org/10.1038/383327a0>
- von Glasow, R., von Kuhlmann, R., Lawrence, M. G., Platt, U., & Crutzen, P. J. (2004). Impact of reactive bromine chemistry in the troposphere. *Atmospheric Chemistry and Physics*, 4, 2481–2497. <https://doi.org/10.5194/acp-4-2481-2004>
- Wagner, N. L., Riedel, T. P., Young, C. J., Bahreini, R., Brock, C. A., Dubé, W. P., et al. (2013). N₂O₅ uptake coefficients and nocturnal NO₂ removal rates determined from ambient wintertime measurements. *Journal of Geophysical Research: Atmospheres*, 118, 9331–9350. <https://doi.org/10.1002/jgrd.50653>
- Wang, X., Jacob, D. J., Eastham, S. D., Sulprizio, M. P., Zhu, L., Chen, Q., et al. (2018). The role of chlorine in tropospheric chemistry. *Atmospheric Chemistry and Physics Discussions*. <https://doi.org/10.5194/acp-2018-1088>
- Wang, X., Wang, H., Xue, L., Wang, T., Wang, L., Gu, R., et al. (2017). Observations of N₂O₅ and ClNO₂ at a polluted urban surface site in North China: High N₂O₅ uptake coefficients and low ClNO₂ product yields. *Atmospheric Environment*, 156, 125–134. <https://doi.org/10.1016/j.atmosenv.2017.02.035>
- Yun, H., Wang, W., Wang, T., Xia, M., Yu, C., Wang, Z., et al. (2018). Nitrate formation from heterogeneous uptake of dinitrogen pentoxide during a severe winter haze in southern China. *Atmospheric Chemistry and Physics*, 18, 17,515–17,527. <https://doi.org/10.5194/acp-18-17515-2018>

References From the Supporting Information

- Bahreini, R., Dunlea, E. J., Matthew, B. M., Simons, C., Docherty, K. S., DeCarlo, P. F., et al. (2008). Design and operation of a pressure-controlled inlet for airborne sampling with an aerodynamic aerosol lens. *Aerosol Science and Technology*, 42(6), 465–471. <https://doi.org/10.1080/02786820802178514>
- Brown, S. S., Dubé, W. P., Peischl, J., Ryerson, T. B., Atlas, E., Warneke, C., et al. (2011). Budgets for nocturnal VOC oxidation by nitrate radicals aloft during the 2006 Texas Air Quality Study. *Journal of Geophysical Research*, 116, D24305.
- Cai, Y., Montague, D. C., Mooiwee-Bryan, W., & Deshler, T. (2008). Performance characteristics of the ultra high sensitivity aerosol spectrometer for particles between 55 and 800 nm: Laboratory and field studies. *Journal of Aerosol Science*, 39(9), 759–769. <https://doi.org/10.1016/j.jaerosci.2008.04.007>
- Day, D. A., Wooldridge, P. J., Dillon, M. B., Thornton, J. A., & Cohen, R. C. (2002). A thermal dissociation laser-induced fluorescence instrument for in situ detection of NO₂, peroxy nitrates, alkyl nitrates, and HNO₃. *Journal of Geophysical Research*, 107(D6), 4046. <https://doi.org/10.1029/2001JD000779>
- DeCarlo, P. F., Kimmel, J. R., Trimborn, A., Northway, M. J., Jayne, J. T., Aiken, A. C., et al. (2006). Field-deployable, high-resolution, time-of-flight aerosol mass spectrometer. *Analytical Chemistry*, 78, 8281–8289. <https://doi.org/10.1021/ac061249n>
- Dibb, J. E., Talbot, R. W., & Scheuer, E. M. (2000). Composition and distribution of aerosols over the North Atlantic during the Subsonic Assessment Ozone and Nitrogen Oxide Experiment (SONEX). *Journal of Geophysical Research*, 105(D3), 3709–3717. <https://doi.org/10.1029/1999JD900424>
- Dibb, J. E., Talbot, R. W., Scheuer, E. M., Blake, D. R., Blake, N. J., Gregory, G. L., et al. (1999). Aerosol chemical composition and distribution during the Pacific Exploratory Mission (PEM) tropics. *Journal of Geophysical Research*, 104(D5), 5785–5800. <https://doi.org/10.1029/1998JD100001>
- Fuchs, H., Dube, W. P., Lerner, B. M., Wagner, N. L., Williams, E. J., & Brown, S. S. (2009). A sensitive and versatile detector for atmospheric NO₂ and NO_x based on blue diode laser cavity ring-down spectroscopy. *Environmental Science & Technology*, 43(20), 7831–7836. <https://doi.org/10.1021/es902067h>
- Hayes, P. L., Ortega, A. M., Cubison, M. J., Froyd, K. D., Zhao, Y., Cliff, S. S., et al. (2013). Organic aerosol composition and sources in Pasadena, California, during the 2010 CalNex campaign. *Journal of Geophysical Research: Atmospheres*, 118, 9233–9257. <https://doi.org/10.1002/jgrd.50530>

- Lee, B. H., Lopez-Hilfiker, F. D., Mohr, C., Kurten, T., Worsnop, D. R., & Thornton, J. A. (2014). An iodide-adduct high-resolution time-of-flight chemical-ionization mass spectrometer: Application to atmospheric inorganic and organic compounds. *Environmental Science & Technology*, 48(11), 6309–6317. <https://doi.org/10.1021/es500362a>
- McNaughton, C., Clarke, A. D., Howell, S. G., Pinkerton, M., Anderson, B., Thornhill, L., et al. (2007). Results from the DC-8 inlet characterization experiment (DICE): Airborne versus surface sampling of mineral dust and sea salt aerosols. *Aerosol Science and Technology*, 41(2), 136–159. <https://doi.org/10.1080/02786820601118406>
- Washenfelder, R. A., Wagner, N. L., Dube, W. P., & Brown, S. S. (2011). Measurement of atmospheric ozone by cavity ring-down spectroscopy. *Environmental Science & Technology*, 45(7), 2938–2944. <https://doi.org/10.1021/es103340u>
- Weinheimer, A. J., Walega, J. G., Ridley, B. A., Gary, B. L., Blake, D. R., Blake, N. J., et al. (1994). Meridional distributions of NO_x, NO_y, and other species in the lower stratosphere and upper troposphere during AASE II. *Geophysical Research Letters*, 21, 2583–2586. <https://doi.org/10.1029/94GL01897>
- Wennberg, P. (1999). Bromine explosion. *Nature*, 397, 299. <https://doi.org/10.1038/16805>